molecular pharmaceutics

pubs.acs.org/molecularpharmaceutics

Article

Transcript-Activated Coatings on Titanium Mediate Cellular Osteogenesis for Enhanced Osteointegration

Omnia Fayed, Martijn van Griensven, Zeinab Tahmasebi Birgani, Christian Plank, and Elizabeth R. Balmayor*

Cite This: *Mol. Pharmaceutics* 2021, 18, 1121−1137

Read Online

ACCESS | Metrics & More | Article Recommendations | Supporting Information

ABSTRACT: Osteointegration is one of the most important factors for implant success. Several biomolecules have been used as part of drug delivery systems to improve implant integration into the surrounding bone tissue. Chemically modified mRNA (cmRNA) is a new form of therapeutic that has been used to induce bone healing. Combined with biomaterials, cmRNA can be used to develop transcript-activated matrices for local protein production with osteoinductive potential. In this study, we aimed to utilize this technology to create bone morphogenetic protein 2 (BMP2) transcript-activated coatings for titanium (Ti) implants. Therefore, different coating methodologies as well as cmRNA incorporation strategies were evaluated. Three different biocompatible biomaterials were used for the coating of Ti, namely, poly-D,L-lactic acid (PDLLA), fibrin, and fibrinogen. cmRNA-coated Ti disks were assayed for transfection efficiency, cmRNA release, cell viability and proliferation, and osteogenic activity *in vitro*. We found that cmRNA release was significantly delayed in Ti surfaces previously coated with biomaterials. Consequently, the transfection efficiency was greatly improved. PDLLA coating improved the transfection efficiency in a concentration-dependent manner. Lower PDLLA concentration used for the coating of Ti resulted in higher transfection efficiency. Fibrin and fibrinogen coatings showed even higher transfection efficiencies compared to all PDLLA concentrations. In those disks, not only the expression was up to 24-fold higher but also the peak of maximal expression was delayed from 24 h to 5 days, and the duration of expression was also extended until 7 days post-transfection. For fibrin, higher transfection efficiencies were obtained in the coatings with the lowest thrombin amounts. Accordingly, fibrinogen coatings gave the best results in terms of cmRNA transfection. All biomaterial-coated Ti surfaces showed improved cell viability and proliferation, though this was more noticeable in the fibrinogen-coated disks. The latter was also the only coating to support significant amounts of BMP2 produced by C2C12 cells *in vitro*. Osteogenesis was confirmed using BMP2 cmRNA fibrinogen-coated Ti disks, and it was dependent of the cmRNA amount present. Alkaline phosphatase (ALP) activity of C2C12 increased when using fibrinogen coatings containing 250 ng of cmRNA or more. Similarly, mineralization was also observed that increased with increasing cmRNA concentration. Overall, our results support fibrinogen as an optimal material to deliver cmRNA from titanium-coated surfaces.

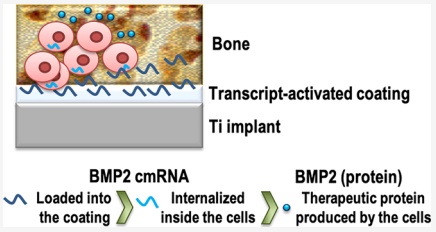

KEYWORDS: *chemically modified mRNA, fibrin, fibrinogen, PDLLA, transcript-activated matrix, implants, bone regeneration*

INTRODUCTION

For decades, biocompatible titanium (Ti) implants have been successfully used to treat and restore hard tissue defects in dentistry and orthopedics.[1,2] Implant integration in the surrounding bone tissue (osteointegration) is one of the most important factors for implant success. Thus, many surface modifications have been introduced on metallic implants to support peri-implant bone formation.[2] Among those, surface functionalization with osteoinductive molecules, for example, proteins, peptides, growth factors, DNA, and enzymes has shown promising results.[3]

Incorporation of osteoinductive molecules on Ti surfaces could be achieved *via* chemical or physical methods. Two main methods have been reported to physically immobilize molecules onto implant surfaces, (i) physical adsorption and (ii) physical entrapment within biodegradable materials.[3] Physical adsorption typically occurs by the formation of weak bonds (*e.g.*, van der Waals or electrostatic forces, hydrogen bonds, or hydrophobic interactions). Thus, it is a weak functionalization method in which particles adsorb and desorb from the metallic surface in an uncontrolled manner. This may lead to the fast release of bioactive molecules. In turn, the probability of side effects due to excessive dose may be increased.[4,5] Nevertheless, physical adsorption is a simple and mild method that does not disrupt the structure of bioactive molecules. Instead, in the physical entrapment approach, a barrier material is used to retain and protect the

Received: October 21, 2020
Revised: January 14, 2021
Accepted: January 14, 2021
Published: January 25, 2021

https://dx.doi.org/10.1021/acs.molpharmaceut.0c01042
Mol. Pharmaceutics 2021, 18, 1121−1137

bioactive molecules on the metallic surface. Depending on the material used to entrap the bioactive molecule, this approach may retain the mildness of the physical adsorption method. It also allows for controlled release, overcoming disadvantages associated with burst release.[3] Many biodegradable, synthetic, and natural polymers have been investigated for physical entrapment.[6−8] Poly(lactide) (PLA) and poly(lactide-*co*-glycolide) (PLGA) are among the best established biodegradable synthetic polymer coatings for metallic implants. They feature high mechanical stability while providing an adequate platform for local controlled release of bioactive molecules.[9−12] Natural polymers such as collagen, silk fibroin, gelatin, fibrin, and fibrinogen have also been researched to be used for coating metallic implants.[13−16] In particular, fibrin and fibrinogen have been used for many tissue engineering applications due to their natural advantage as the primary healing scaffold in the body.[17] They provide support for cell adhesion, migration, and differentiation. These materials also support extracellular matrix deposition and cell−cell interactions as part of their natural function.[18] Therefore, they are good candidates for a coating material to entrap bioactive molecules.

Several bioactive molecules have been investigated for osteoinductivity.[19,20] Some have shown suitability for metallic implant incorporation. Relevant examples include alginylglycylaspartic acid, collagen type I, and growth factors such as fibroblast growth factor 2, transforming growth factor-β 2, and bone morphogenetic proteins.[20] Among them, bone morphogenetic protein 2 (BMP2) has shown positive clinical results for bone healing.[15,21] Although the local administration of BMP2 has been approved by the Food and Drug Administration (FDA), its routine clinical use remains limited. This can be attributed to difficulties restricting the protein activity to the area of application, its short half-life *in vivo*, and its high cost.[12,22] Several delivery matrices for recombinant BMP2 have been developed.[23−25] Yet, there is substantial potential for improvement toward clinical applications.

Gene therapy may be an alternative to bone regeneration.[26] Gene delivery, which provides the gene encoding the protein rather than a degradable protein, is effective but very difficult to translate into human clinical use. In recent years, messenger RNA (mRNA) has emerged as a promising alternative to plasmid DNA for gene delivery. Delivering mRNA poses several advantages. For example, mRNA does not require crossing the nuclear membrane to exert its function, which is advantageous to non-dividing cells also. Moreover, mRNA is considered safer due to its lack of integration into the genome and its relatively short half-life of the transfected cells.[27−29] Added to that, the production of desired mRNAs by *in vitro* transcription (IVT) is relatively easy.[29] In line with that, using modified nucleotides during mRNA production can substantially reduce its immunogenicity and improve the stability.[30] Local delivery of mRNA (transcripts) can be achieved using non-viral vectors, which represent another safety advantage over viral gene therapy. Numerous studies have established lipids as efficient non-viral vectors for mRNA delivery.[31−33] In our previous work, we have demonstrated the effectiveness of chemically modified mRNA (cmRNA)−lipid complexes *in vitro* in promoting osteogenic differentiation of mesenchymal stem cells[27,34,35] and *in vivo* in inducing bone healing in non-critical[27,36] as well as critical-sized bone defects.[35]

In the present study, we aimed to utilize the cmRNA technology to create BMP2 transcript-activated coatings for titanium (Ti) implants. We evaluated different Ti surface functionalization approaches as well as cmRNA incorporation strategies. The effect of these approaches on the cmRNA transfection efficiency and kinetics, cell viability and proliferation, and osteogenic differentiation was studied using NIH3T3 and C2C12 cells. We hypothesize that the entrapment of cmRNA−lipid complexes within a biocompatible matrix subsequently coated on Ti implants may be beneficial for cellular and bone regeneration outcomes. In particular, osteogenic differentiation of cells surrounding the implant may improve its integration in an *in vivo* orthotopic scenario.

EXPERIMENTAL METHODS

cmRNA Preparation. cmRNAs that code for *Metridia* luciferase (MetLuc) and BMP2 were used in this work. MetLuc is a secreted luciferase that allows the analysis of its expression in cell culture supernatants. In this study, MetLuc was selected as a model for a secreted therapeutic protein also, that is, BMP2. BMP2 was selected as a molecule to produce an osteoinductive cmRNA due to its known bone induction potential. Moreover, BMP-2 is FDA-approved and frequently used in clinic to treat bone fractures and non-union defects.

cmRNAs were synthesized *via* IVT according to the method previously described by our group.[35] In brief, the corresponding plasmids were added to a mixture of ribonucleotides and T7 RNA polymerase (Thermo Fisher Scientific Baltics UAB, Lithuania). The ribonucleotide mixture was prepared containing chemically modified ribonucleotides. For MetLuc cmRNA, 25% of 5-methylcytidine-5′-triphosphate and 25% of 2-thiouridine-5′-triphosphate were used to replace their non-modified counterparts during IVT. For BMP2 cmRNA, 35% of 5-iodo-uridine and 7.5% of 5-iodo-cytidine were used. The chemically modified nucleotides were obtained from Jena Bioscience GmbH, Germany. In addition, an anti-reverse cap analogue (Jena Bioscience GmbH, Germany) was added to the mixture. After the IVT reaction was concluded, DNase was added to degrade the plasmid template. The resulting MetLuc transcript was subjected to enzymatic 3′-polyadenylation, while the BMP2 transcript had the poly-A tail encoded into the used plasmid template (200 nucleotides in length). The transcripts were purified by ammonium acetate precipitation and resuspended in water for injection. The cmRNA concentration was measured using a NanoDrop 2000C spectrophotometer (Thermo Fisher Scientific, USA). The cmRNA quality and integrity were assessed by automated capillary electrophoresis (Fragment Analyzer, Agilent Technologies, USA). HPLC (Agilent 1260 Infinity, Agilent Technologies, USA) was performed for nucleotide analysis. As additional quality control check, the produced cmRNAs were tested for transfection ability of NIH3T3 cells using Lipofectamine 2000 (Supporting Information).

Lipoplex Formulation and Characterization. A non-viral lipidoid vector was formulated using a cationic lipidoid with dipalmitoyl phosphatidylcholine, cholesterol helper lipids, and 1,2-dimyristoyl-*rac*-glycero-3-methylpolyoxyethylene PEGylated lipid.[31] Lipoplexes, that is, lipid−cmRNA complexes, were formulated utilizing the solvent-exchange method.[37] In brief, an ethanol or isopropanol solution containing lipids was rapidly injected into an aqueous buffered solution of cmRNA (10 mM citrate buffer/150 mM sodium chloride). The mixture was then vortexed for 15 s and incubated at RT for 30 min to form the complexes. To remove the excess of isopropanol, the lipoplexes were dialyzed

https://dx.doi.org/10.1021/acs.molpharmaceut.0c01042
Mol. Pharmaceutics 2021, 18, 1121−1137

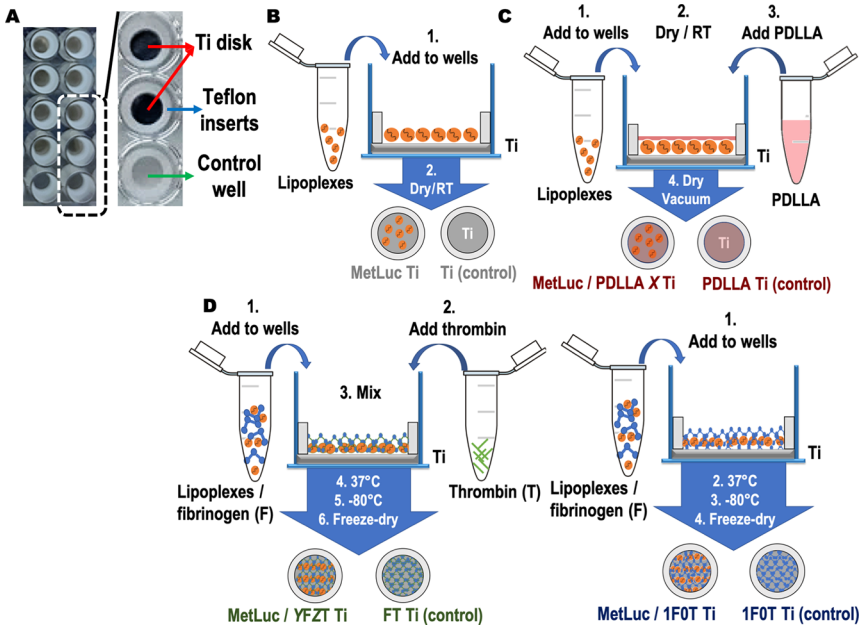

Figure 1. Schematic representation of the experimental setup used for incorporation of cmRNA onto Ti disks. Of note, the diagrams used in this scheme are not a true representation of the exact plasticware dimensions used during the experiments. (A) Surface coating and cellular experiments were performed using 96-well plates. An image of 10 of the wells was taken for illustration purposes. Furthermore, a magnified image showing three wells is provided for a more detailed illustration. Ti disks were placed inside the wells of a 96-well plate. Teflon ring inserts were used to keep the Ti disks in place. (B) cmRNA incorporation on Ti surface *via* physical adsorption. Drawings of two representative wells are shown indicating the sample and the control for this experiment (C) cmRNA incorporation *via* physical adsorption with subsequent deposition of a PDLLA protective layer; *X* represents different PDLLA concentrations (0.25, 0.5, 1, 2, and 3 mg/disk). Drawings of two representative wells are shown indicating the sample and the control for this experiment (D) cmRNA incorporation on the Ti surface *via* physical entrapment with fibrin and fibrinogen. Left drawing showing fibrin entrapment, in which cmRNA lipoplexes were mixed with fibrinogen and immediately deposited onto the Ti disks. Subsequently, an equal volume of thrombin solution was added to the fibrinogen cmRNA mixture. *YFZT* indicates the composition of the fibrin coating: *Y* indicates the amount of fibrinogen (F) and *Z* indicates the amount of thrombin (T). The right drawing shows fibrinogen entrapment. Here, the cmRNA lipoplexes were mixed with fibrinogen and deposited on the surface of Ti. 1F0T indicates that no thrombin was added. Drawings of two representative wells are shown indicating the sample and the control for this experiment.

overnight against double distilled water (ddH_2O) using a dialysis membrane (7 kDa cutoff molecular weight, Thermo Fisher Scientific, USA). The final cmRNA concentration in the formulated lipoplexes was 100 μg/mL with an N/P ratio of 8.

The size and zeta potential of lipoplex particles were measured *via* dynamic light scattering (Malvern Zetasizer Nano ZS, UK). Moreover, these determinations were performed daily for up to 7 days after lipoplex formation. In short, the formed MetLuc cmRNA and BMP2 cmRNA lipoplexes were incubated at 37 °C. An individual sample was used for each time of observation. In addition, samples corresponding to blank (lipid solution) and control (*i.e.*, freshly formed cmRNA lipoplex) were also analyzed. Size and zeta potential analysis was performed at RT using water for injection (pH = 5.5).

To determine the complexation efficiency, concentrations of cmRNAs before (t_0) and after (t_x) lipoplex formation were determined. Complexation efficiency was analyzed over time. For this, MetLuc cmRNA and BMP2 cmRNA lipoplexes were incubated at 37 °C for up to 7 days. Samples were collected daily to measure cmRNA concentrations after lipoplex formation. In order to release the cmRNA from the lipid complexes (and thus free for detection), treatment with a detergent solution was performed. The solution was composed of a 1:14 heparin and Triton X-100 mixture. The heparin used was 40 mg/mL prepared in ddH_2O. The detergent solution was mixed 1:1 (v/v) with diluted lipoplex samples. The mixture was incubated at 70 °C for 10 min under gentle shaking (300 rpm). Next, the mixture was centrifuged for 1 min to recollect the condensed droplets.

For quantification, a Quant-iT RiboGreen RNA assay kit (Thermo Fisher, USA) was used following the manufacturer's instructions. Complexation efficiency was calculated as follows

$$\%\ \text{complexation efficiency} = \frac{\text{cmRNA amount}_{\text{in lipoplex}(t_x)}}{\text{cmRNA amount}_{\text{used for lipoplex}(t_0)}} \times 100$$

Furthermore, the integrity of cmRNAs released from the lipoplexes was analyzed using an automated capillary electrophoresis system (Fragment Analyzer, Advanced Analytical, USA). This analysis was performed daily for up to 7 days.

Finally, the produced lipoplexes were tested for transfection ability using NIH3T3 cells. Transfections were performed in triplicate using 0.025 ng of cmRNA/cell. Expression of MetLuc and BMP2 was assessed following the methodology described hereafter. For storage purposes, the lipoplexes were aliquoted and freeze-dried using 5% trehalose (Sigma-Aldrich, USA) as a cryopreservant.

Preparation of Ti Disks for cmRNA Coating. Ti foils (Ti grade IV, thickness = 50 μm, ANKURO Int. GmbH, Germany) were cut into 6 mm diameter circular disks to fit inside the wells of a 96-well plate. The disks were degreased in 99.7% acetone (Carl Roth, Germany) for 10 min at RT in an ultrasonic bath. Next, the disks were washed three times, first in ddH_2O and then in ethanol 80%. The last ethanol wash was

https://dx.doi.org/10.1021/acs.molpharmaceut.0c01042
Mol. Pharmaceutics 2021, 18, 1121−1137

Table 1. Experimental Conditions Used for cmRNA Incorporation on Ti[a]

sample (Ti disk)	cmRNA	cmRNA (ng/disk)	cmRNA (ng/mm^2 disk)	coating methodology	material		
					coating material	concentration (mg/disk)	ratio (F/T)
MetLuc	MetLuc cmRNA	62.5	3.2	physical adsorption	none	n.a.	n.a.
		125	6.4				
		250	12.8				
		500	25.5				
MetLuc/PDLLA 0.25	MetLuc cmRNA	500	25.5	physical adsorption—PDLLA protective layer	PDLLA	0.25	n.a.
MetLuc/PDLLA 0.5						0.5	
MetLuc/PDLLA 1						1	
MetLuc/PDLLA 2						2	
MetLuc/PDLLA 3						3	
MetLuc/1F1T	MetLuc cmRNA	500	25.5	physical entrapment	fibrinogen	n.a.	1:1
MetLuc/1F0.5T							1:0.5
MetLuc/1F0.25T					thrombin		1:0.25
MetLuc/1F0T							1:0
BMP2/1F1T	BMP2 cmRNA	62.5	3.2	physical entrapment	fibrinogen	n.a.	1:1
		125	6.4				
		250	12.8		thrombin		
		500	25.5				
BMP2/1F0T	BMP2 cmRNA	62.5	3.2	physical entrapment	fibrinogen	n.a.	1:0
		125	6.4				
		250	12.8				
		500	25.5				
BMP2/PDLLA 0.25	BMP2 cmRNA	500	25.5	physical adsorption—PDLLA protective layer	PDLLA	0.25	n.a.
BMP2	BMP2 cmRNA	500	25.5	physical adsorption	none	n.a.	n.a.

[a]Overview of developed cmRNA Ti disks using PDLLA, fibrin, or fibrinogen as a coating biomaterial. Abbreviations: Ti, titanium; cmRNA, chemically modified mRNA; PDLLA, poly-D,L-lactic acid; MetLuc, *Metridia* luciferase; BMP2, bone morphogenetic protein 2; *YFZT*, where *Y* indicates the amount of fibrinogen, F, and *Z* indicates the amount of thrombin, T.

performed in an ultrasonic bath (10 min at RT). The excess ethanol was removed and the disks were left to air-dry inside a laminar flow cabinet. Sterilized disks were kept in an air-tight container until further use.

Experimental Setup Used for cmRNA Coating. Teflon circular ring inserts were used to keep the Ti disks in place inside the 96-well plate. The coating was confined to the exposed Ti surfaces, as shown in Figure 1A. The ring inserts were made using polytetrafluoroethylene Teflon 3D printer tubes (StickandShine, Germany). The dimensions of the rings were the following: outer diameter = 7 mm, inner diameter = 5 mm, and height = 2 mm. The rings were degreased with acetone 99.7%, washed three times with ddH_2O and three times with ethanol 80%, and then finally autoclaved to be sterilized. To prepare the Ti disks for further coating and cellular experiments, the disks were placed in a 96-well plate and subsequently fixed using the ring inserts (Figure 1A). Next, the plates were irradiated with ultraviolet light for 1 h to be sterilized. Meaningfully, the Ti disks and Teflon ring inserts showed to be a highly stable system that remained in place with no floating or flipping of the samples during experimentation.

Ti Coating *via* Physical Adsorption. Sterilized Ti disks were physically coated by addition of 30 μL of MetLuc cmRNA lipoplexes dispersed in 20% v/v ethanol solution. Several cmRNA concentrations, in the range of 500−62.5 ng/disk were used for the coating. This cmRNA concentration screening was performed to determine the optimal cmRNA concentration/disk in terms of transfection efficiency. Next, cmRNA-coated disks were allowed to air-dry overnight inside the laminar flow cabinet. A schematic representation of the coating procedure is shown in Figure 1B. Also, a sample overview is presented in Table 1. The samples coated following this methodology will be termed hereafter MetLuc Ti disks.

Ti Coating *via* Physical Adsorption and Using a Poly-D,L-lactic Acid Protective Layer. A cmRNA concentration of 500 ng/disk was selected to perform the coating using poly-D,L-lactic acid (PDLLA; Resomer R 203 H, Sigma-Aldrich, USA). First, Ti disks were coated with MetLuc cmRNA lipoplexes, as described in the previous section. Then, a layer of PDLLA was deposited onto the dried MetLuc cmRNA-coated Ti disks. To achieve this, PDLLA was dissolved in ethyl acetate (99.8%, Sigma-Aldrich, USA). Different PDLLA concentrations (*i.e.*, 0.25, 0.5, 1, 2, and 3 mg/disk) were used for the coating.[12] Thereafter, the cmRNA/PDLLA-coated Ti disks were left to air-dry under the laminar cabinet for 3 h with a subsequent step of vacuum-drying (500 Torr) in a closed desiccator for 1 h. The coating procedure and PDLLA layer deposition were performed at RT. In addition, control samples were produced by depositing a PDLLA layer on Ti disks without previous cmRNA coating. Thus, the corresponding controls had the same polymeric coating, but did not contain

https://dx.doi.org/10.1021/acs.molpharmaceut.0c01042
Mol. Pharmaceutics 2021, 18, 1121−1137

MetLuc cmRNA lipoplexes. A schematic representation of the coating procedure and PDLLA layer deposition is illustrated in Figure 1C and a sample overview is presented in Table 1. The samples coated using the PDLLA protective layer will be termed hereafter MetLuc/PDLLA *X* Ti disks, where *X* indicates the different PDLLA concentrations used for the coating.

Ti Coating *via* Physical Entrapment Using Fibrin and Fibrinogen. For this experiment, Tissucol (Baxter, Austria) was used as a fibrin source. The components of the kit are fibrinogen (66 mg/mL) and thrombin (100 IU/mL). MetLuc cmRNA lipoplexes were mixed with fibrinogen and immediately deposited onto the Ti disks using 15 μL per disk. Care was placed to ensure a homogeneous distribution on the surface of the disks. Next, an equal volume of thrombin solution was added to the fibrinogen−cmRNA mixture and mixed gently to allow for coagulation to start on the disk's surface. The fibrin-coated Ti disks were then incubated for 30 min inside a cell culture incubator (5% CO_2 and 37 °C). This ensured complete coagulation and fibrin gel formation. After incubation, the fibrin-coated samples were frozen for 1 h at −80 °C and then freeze-dried (Alpha 2-4, Martin Christ, Germany) for 48 h. The primary drying cycle was performed for the first 24 h using a shelf-temperature of −30 °C and a vacuum of 0.05 mbar. A secondary drying was done for the final 24 h at 4 °C and 0.025 mbar vacuum. The concentration of cmRNA used was 500 ng/disk. The coating steps are illustrated in Figure 1D. The plates containing the ready-to-use samples were vacuum-sealed and stored at 4 °C until further use.

To evaluate the effect of fibrin composition on the coating performance, the amount of thrombin was reduced during gel formation. Thus, different fibrinogen (F) to thrombin (T) ratios, that is, 1:1, 1:0.5, 1:0.25, and 1:0 (v/v) were used. Therefore, a set of samples was generated, that will be termed hereafter MetLuc/*Y*F*Z*T Ti disks, where *Y* indicates the amount of fibrinogen F = 1 and *Z* indicates the amount of thrombin T. Thus, a sample was obtained that was coated with fibrinogen only (*i.e.*, F/T = 1:0 or 1F0T, Figure 1D right drawing). A sample overview is presented in Table 1. In addition, control samples were produced by forming the fibrin gel (different compositions) but without previous cmRNA addition.

Morphological Characterization of Ti Coatings. The surface profile of different coatings developed in this study was studied using a confocal laser scanning microscope-based profilometer (VK-X250, KEYENCE, Japan) in combination with its MultiFileAnalyzer analysis software (KEYENCE, Japan). To determine the surface roughness, three regions of interest (ROI) and four lines of interest (LOI) were selected per sample. ROI and LOI were used to calculate the arithmetic mean heights over surface (Sa) and over line (Ra), respectively. In addition, the surface of the coatings was imaged using a scanning electron microscope (Teneo, FEI, USA) at a magnification of 2000X, an accelerating voltage of 2 keV, and a working distance of approximately 10 mm. Prior to SEM imaging, the samples were sputter-coated with a gold layer (SC7620, Quorum, UK) for increasing the surface conductivity.

Incorporation of BMP2 cmRNA into Ti Coatings. In order to coat the Ti disks with BMP2 cmRNA, the best coating methodologies were selected from the above-described ones. High transfection efficiency and good cell compatibility were the main parameters considered for the selection. Thus, fibrinogen [F/T ratio: 1:0 (v/v)], fibrin [F/T ratio: 1:1 (v/v)], and PDLLA (0.25 mg PDLLA/disk) coatings were performed. Moreover, uncoated Ti (cmRNA incorporated *via* physical adsorption onto the metallic surface) was prepared and used as control. The concentration of BMP2 cmRNA used was 500 ng/disk. The obtained samples will be termed hereafter BMP2/1F0T Ti disks (fibrinogen), BMP2/1F1T Ti disks (fibrin), BMP2/PDLLA 0.25 Ti disk (PDLLA), and BMP2 Ti disks (Ti only). A sample overview is presented in Table 1.

BMP2 Release from BMP2 cmRNA-Coated Ti Disks. BMP2/1F0T (fibrinogen), BMP2/1F1T (fibrin), BMP2/PDLLA 0.25, and BMP2 Ti disks were incubated in Dulbecco's modified Eagle's medium (DMEM, Sigma-Aldrich, USA) supplemented with 1% penicillin/streptomycin (P/S, Sigma-Aldrich, USA) antibiotics and without serum at 37 °C for up to 7 days. The supernatants were collected after 2 h and then daily for up to 7 days. In addition, a sample was collected on days 10 and 14 to confirm whether BMP2 cmRNA could be detected in the supernatants at prolonged releasing times. The samples were immediately frozen at −80 °C until further analysis. Fresh DMEM was added to the Ti disks to maintain a volume of 200 μL during the release experiment. At day 7, disks in which the cmRNA was entrapped within a 3D matrix (*i.e.*, BMP2/1F1T and BMP2/1F0T Ti disks) were digested to investigate whether cmRNA was still present inside the matrix. Therefore, disks were harvested, washed with PBS and digested with 0.05% trypsin (Thermo Fisher, USA) by incubating the samples at 37 °C for 1 h. The digested samples were also collected for analysis.

cmRNA was quantified in the supernatants and digested samples after treatment with a heparin/Triton X-100 detergent solution. For quantification, the Quant-iT RiboGreen RNA assay kit was used following the instructions of the manufacturer. Details on both methods, detergent treatment, and RiboGreen quantification can be found in previous sections. Measurements were performed using a microplate reader (Tecan, Infinite M200 PRO, Switzerland). The results were reported as percent of control (*i.e.*, fresh lipoplexes containing 500 ng of BMP2 cmRNA) corresponding to the initial amount of cmRNA incorporated into the coating.

Cell Culture. The NIH3T3 cell line (mouse embryonic fibroblasts, ATCC CRL-1658) was used for transfections on MetLuc cmRNA-coated Ti disks. It is known that mRNA transfections of NIH3T3 cells are reproducible and result in elevated expression levels. Thus, this cell line was used to initially evaluate the transfection efficiency using the different coating methodologies previously described. NIH3T3 cells were cultured in DMEM containing 4.5 g/L glucose and 0.584 g/L L-glutamine (Sigma-Aldrich, USA). DMEM was supplemented with 10% fetal bovine serum (FBS) and 1% P/S, both from Sigma-Aldrich, USA.

The C2C12 cell line (mouse muscle myoblast, ATCC CRL-1772) was used for transfections on BMP2 cmRNA-coated Ti disks. This cell line is able to differentiate into osteoblasts in the presence of recombinant BMP2.[38] Therefore, this cell line was selected to functionally evaluate possible differentiation due to cell-produced BMP2 as a result of cmRNA transfection. C2C12 cells were cultured in DMEM containing 4.5 g/L glucose, 0.584 g/L L-glutamine (Sigma-Aldrich, USA), supplemented with 10% FBS and 1% P/S. This culture medium was also used during BMP2 transfection experiments. However, for the *in vitro* differentiation experiments, low

https://dx.doi.org/10.1021/acs.molpharmaceut.0c01042
Mol. Pharmaceutics 2021, 18, 1121−1137

glucose DMEM (1 g/L glucose and 0.584 g/L L-glutamine) was used after supplementation with 2% FBS, 1% P/S, 10 mM β-glycerophosphate (AppliChem, Germany), and 200 μM ascorbic acid (Sigma-Aldrich, USA). The cells were cultured and kept at 37 °C in a humid 5% CO_2 cell culture incubator.

Cell Transfection on MetLuc cmRNA-Coated Ti Disks. For transfection, NIH3T3 were seeded at 10^4 cells/disk in a 96-well plate. The disks were coated with MetLuc cmRNA using each of the coating methodologies described before. As previously mentioned, cmRNA concentrations were in the range of 500−62.5 ng/disk depending on the coating methodology utilized. This means that 50−6.25 pg cmRNA/cell were tested for transfection efficiency. Cell-seeded disks were cultured for up to 10 days at 37 °C in a humidified 5% CO_2 cell culture incubator.

In our study, 100 μL of the cell culture supernatant were collected daily starting 24 h after seeding the cells on MetLuc cmRNA-coated Ti disks. The medium collection continued for up to 7 (PDLLA) or 10 (fibrinogen and fibrin) days depending on the coating type. The same volume of fresh medium was added after each collection. Collected supernatants were frozen at −20 °C until further MetLuc analysis. MetLuc expression was measured by adding 20 μL of 0.05 mM coelenterazine (Synchem, Germany) to 50 μL of the collected supernatant in CoStar white 96-well plates. Luminescence was measured using a microplate reader (Tecan, infinite M200 PRO, Switzerland). For data treatment, supernatants collected from cells seeded on coated Ti disks without cmRNA, that is, untransfected cells, were considered as blank sample. The obtained values were corrected to the total volume (100 μL) and the results are reported in relative light units.

Cell Viability and Proliferation after Transfection with MetLuc cmRNA-Coated Ti Disks. Cell viability was assayed by Alamar Blue. Therefore, cell seeding was performed as previously described and observation times were set to 1, 3, 7, and 14 days post-transfection. Thereafter, the cell culture medium was removed from each well and replaced with 10% alamarBlue solution (MyBioSource, USA) prepared in cell culture medium. Next, the cell culture plates were incubated for 3 h at 37 °C and 5% CO_2 in a humidified incubator. The content of each well was rapidly transferred to a black 96-well plate (Thermo Fisher, USA). Fluorescence was measured at the excitation wavelength of 544 nm and the emission wavelength of 590 nm using a FLUOStar Omega plate reader (BMG Labtech, Germany). As positive control, cells seeded directly on the 96-well plate (in the presence of Teflon inserts) were used (Figure 1A). Moreover, alamarBlue solution (*i.e.*, 10% prepared in cell culture medium) incubated under the same conditions as the samples was used as blank. The values obtained for the blank were deducted from all samples, and activity (%) was calculated as follows

$$\text{activity (\% of positive control)} = \frac{(\text{fluorescence value}_{\text{sample}} - \text{fluorescence value}_{\text{blank}})}{(\text{fluorescence value}_{\text{positive control}} - \text{fluorescence value}_{\text{blank}})} \times 100$$

After alamarBlue assessment, samples were recovered, washed three times with PBS, and used to evaluate cell proliferation. PicoGreen assay, a method based on the determination of double-stranded DNA (dsDNA), was used for this purpose. For this, the Quant-iT PicoGreen dsDNA assay kit (Molecular Probes-Life Technologies, USA) was used. After washing the cells, the Ti disks were carefully removed from the plates and transferred to a separate Eppendorf tube. Then, 250 μL of ddH_2O was added and the samples were frozen at −80 °C. Frozen samples were exposed to three cycles of freezing and rapid thawing at 37 °C in a water bath. Thereafter, the tubes containing the samples were vortexed to break down the cells with subsequent DNA release. From each sample, 50 μL was used to determine the dsDNA concentration. The assay was performed following the manufacturer's instructions. The results were calculated according to the standard curve in dsDNA pg/mL. Also, the total volume of samples, that is, 250 μL, was taken into consideration. Both, alamarBlue and PicoGreen assays were done in triplicate. Moreover, these assays were repeated at least twice to guarantee technical replicates. Relevantly, in both assays, cells seeded on plain Ti disks (*i.e.*, disks with no biomaterial coating and no cmRNA loading) were used as material control. The obtained data were normalized to this control.

Cell Transfection on BMP2 cmRNA-Coated Ti Disks. For transfection, C2C12 were seeded at 10^4 cells/disk in a 96-well plate. The disks were coated with BMP2 cmRNA *via* physical entrapment using fibrinogen or fibrin, as described before. cmRNA concentrations used were 250 ng/disk and 500 ng/disk, respectively. Thus, 25 pg cmRNA/cell and 50 pg cmRNA/cell were administered, respectively. Cell-seeded disks were cultured for up to 4 days at 37 °C in a humidified 5% CO_2 cell culture incubator. As previously described, transfections were performed in DMEM supplemented with 10% FBS and 1% P/S. The supernatants were collected daily for ELISA measurements to measure cell-produced BMP2. BMP2 amounts were determined using human BMP2 ELISA kits (R&D Systems, USA) following the manufacturer's instructions. The experiment was done using biological triplicates and independently repeated at least three times.

Alkaline Phosphatase Activity of C2C12 Transfected on BMP2 cmRNA-Coated Ti Disks. Alkaline phosphatase (ALP) activity was measured, as a first indication of osteogenic differentiation, on days 5, 7, and 10 after C2C12 cells were seeded onto the BMP2/1F0T Ti and BMP2/1F1T Ti disks. In this case, the functionality of all four cmRNA concentrations initially screened for expression (*i.e.*, in the range of 500−62.5 ng/disk) was evaluated. These experiments were conducted in low-glucose, low-serum (*i.e.*, 2% FBS) cell culture medium. Also, β-glycerophosphate and ascorbic acid were added to guarantee the occurrence of ECM deposition and mineralization under the BMP2 stimulus.[39] A medium control consisting of cells seeded on tissue culture plastic and cultured in this supplemented medium was routinely carried out in all the experiments. This sample was systematically evaluated for ALP to rule out a possible medium stimulation.

To assess ALP, the method described by Katagiri *et al.* was modified to meet our setup requirements.[40] In brief, the culture medium was removed from the plates and cells were washed three times with PBS. Next, the samples were frozen at −80 °C until further processing. After thawing, 50 mM Tris−HCl containing 0.1% Triton X-100 buffer (pH 7.5) was added to the samples and the plates were shaken for 20 min. Thereafter, 25 μL of cell lysate was transferred to a new 96-well plate. Next, 100 μL of 10 mM 4-nitrophenyl phosphate disodium salt hydrate (pNPP, Sigma-Aldrich, USA) was added. To prepare the pNPP solution, the salt was dissolved in ALP buffer (*i.e.*, 50 mM glycine and 100 mM Tris-base containing 2 mM $MgCl_2$, and pH was adjusted to 10.5 with NaOH). The

https://dx.doi.org/10.1021/acs.molpharmaceut.0c01042
Mol. Pharmaceutics 2021, 18, 1121−1137

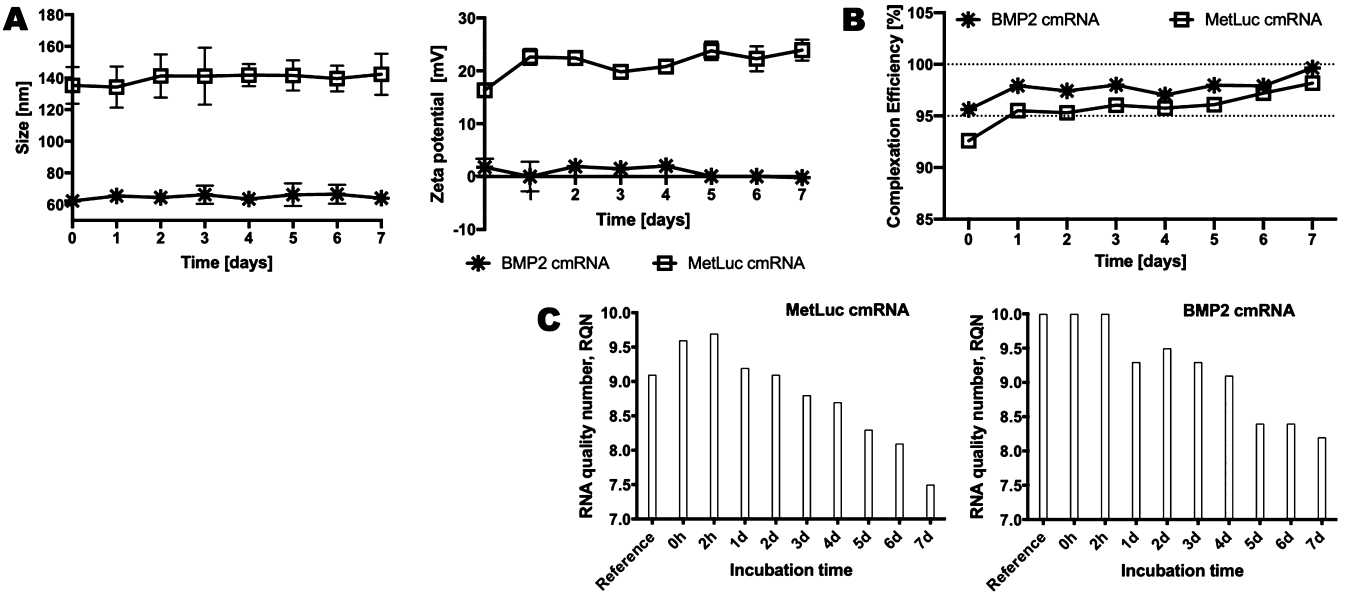

Figure 2. MetLuc cmRNA and BMP2 cmRNA lipoplex characterization. (A) Size and zeta potential over time after lipoplex formation. Multiple, unpaired *t*-test corrected for multiple comparisons by a Holm−Sidak method was performed for data analysis. (B) Complexation efficiency of cmRNA in the lipidoid particles using a non-viral cationic lipid vector. Complexation efficiency is shown over time. (C) Integrity of MetLuc cmRNA and BMP2 cmRNA after complexation. cmRNA was released from the lipidoid particles by heparin−Triton treatment prior to integrity analysis by HPLC. A reference sample was used that consisted of freshly prepared cmRNA complexes. The results are plotted over time after lipoplex formation.

mixture was incubated at RT for 1 h and then quenched with 0.2 M NaOH. The absorbance was measured at 405 nm wavelength using the Tecan microplate reader mentioned previously. The ALP activity was calculated according to a *p*-nitrophenol (*p*NP, Sigma-Aldrich, USA) standard curve. To obtain the standard curve, *p*NP solutions of known concentrations were prepared in ALP buffer. The results are reported in *p*NP concentrations per time unit (μmol/mL/h). Furthermore, the obtained results were normalized to the Ti material control described previously. The experiment was done using quadruplets and independently repeated twice.

Alizarin Red Staining and Quantification. To detect calcium deposits, C2C12 cells were seeded on BMP2/1F0T Ti disks and BMP2/1F1T Ti disks following the same seeding and culture procedures previously described for ALP. Similarly, cmRNA amounts in the range of 500−62.5 ng/disk were investigated. Furthermore, the obtained results were normalized to the Ti material control. This control was also used to confirm the absence of mineralization produced by plain Ti. For Alizarin Red, the observation time was set to 35 days to ensure the occurrence of matrix deposition *in vitro*. Alike the ALP assay, a medium control was evaluated for mineralization to exclude a possible medium stimulation.

For the assay, cells were fixed using ice-cold 96% ethanol for 30 min. Next, Alizarin Red staining solution 0.5% (Sigma-Aldrich, USA) was added and samples were incubated for 10 min. Thereafter, cells were washed five times for 5 min with ddH_2O to remove the excess of Alizarin Red. For quantification, the dye was retrieved using 10% hexadecylpyridinium chloride (Sigma-Aldrich, USA) solution. To ensure complete dye extraction, samples were incubated for 1.5 h. The solution was then transferred to a new 96-well plate and the absorbance was measured at 562 nm wavelength using the Tecan microplate reader. The results were calculated from the Alizarin Red dye standard curve. This experiment was done in quadruplet and independently repeated twice.

Statistical Analysis. Statistical analysis was done using GraphPad Prism version 7.00 software (GraphPad, USA). Multiple comparisons between groups were done using either one-way or two-way analysis of variance (ANOVA) with Tukey's correction and 95% confidence intervals (CIs). In addition, a comparison of two groups over time was performed using multiple *t*-test corrected with Holm−Sidak. Outlier values were identified *via* the "identify outliers" function in software using the ROUT method, which can identify any number of outliers with the Q value set to 10%. The sample size (n) varies between different assays. A minimum of $n = 3$ and a maximum of $n = 8$ replicates were used throughout the entire study. Moreover, experiments were independently repeated, at least twice, to ensure reproducibility. This is mentioned in the "Experimental Methods" section and in the figures of each particular experiment. $p > 0.05$ was considered not significant. Moreover, p values were reported using the GraphPad style as follows: $p \leq 0.05$ was indicated with *, $p \leq 0.01$ was indicated with **, $p \leq 0.001$ was indicated with ***, and $p \leq 0.0001$ was indicated with ****.

RESULTS

cmRNA Coding for MetLuc and BMP2. Two different cmRNA molecules that coded for MetLuc and BMP2, respectively, were obtained. The fragment analysis of both produced cmRNAs indicated adequate integrity, no degradation, and no additional byproducts (Figure S1 of the Supporting Information). Additionally, the peaks corresponded with the expected number of nucleotides for each cmRNA. Moreover, the nucleotide analysis showed proper capping efficiency and incorporation rate of the modified nucleotides. Transfections of NIH3T3 cells in the monolayer with the

https://dx.doi.org/10.1021/acs.molpharmaceut.0c01042
Mol. Pharmaceutics 2021, 18, 1121−1137

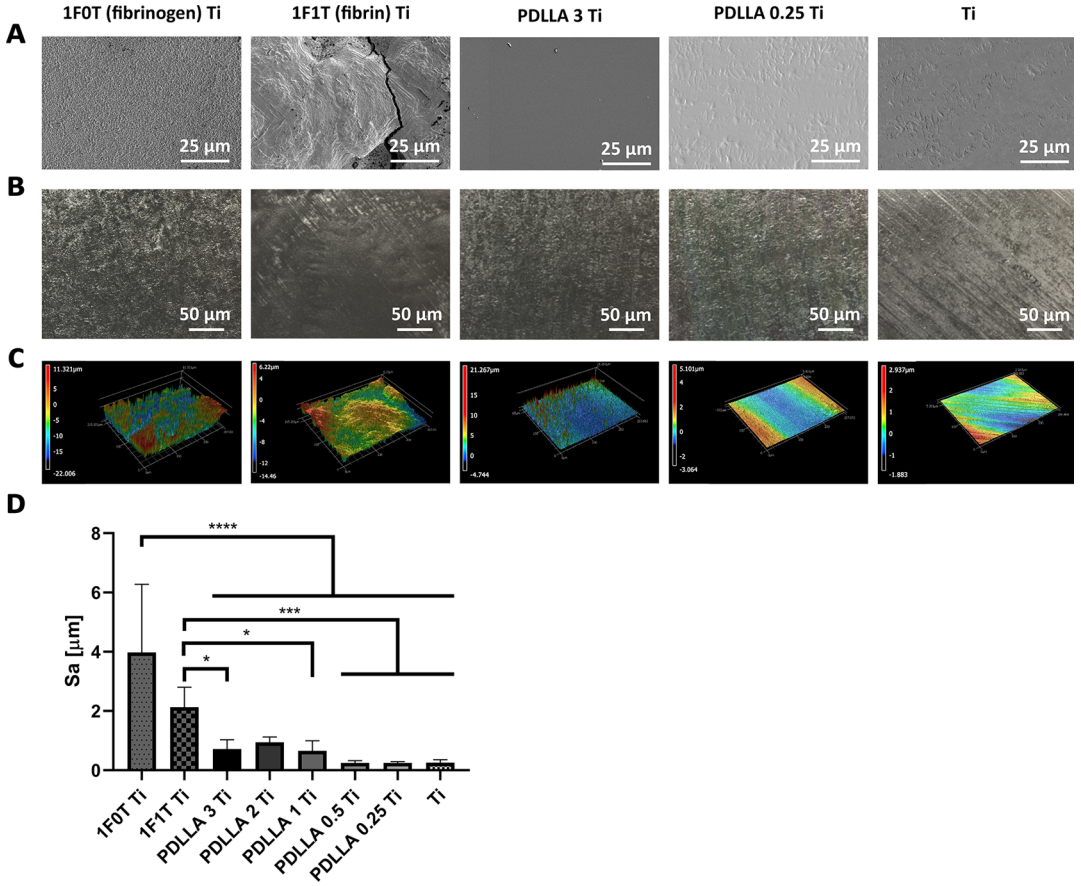

Figure 3. Morphological characterization of polymer coatings on Ti disks. (A) SEM images, (B) laser profilometer images, and (C) height profiles. From left to right, 1F0T Ti disks (fibrinogen), 1F1T Ti disks (fibrin), PDLLA 3 Ti disks (3 mg/disk), PDLLA 0.25 Ti disks (0.25 mg/disk), and Ti disks (uncoated). (D) Quantification of arithmetic mean heights over surface (Sa) for all analyzed Ti disks. Multiple comparisons between groups were analyzed using one-way ANOVA with Tukey's correction and 95% CIs. *$p \leq 0.05$, ***$p \leq 0.001$, and ****$p \leq 0.0001$.

obtained cmRNAs using Lipofectamine 2000 showed effective protein translation (Figure S2 of the Supporting Information).

cmRNA Lipoplexes: Characterization, Stability, and Coating Incorporation. cmRNA lipoplexes featuring the average size (*i.e.*, hydrodynamic diameter) of 135.3 ± 11.6 nm for MetLuc and 62 ± 2 nm for BMP2 cmRNAs were obtained successfully. MetLuc cmRNA lipoplexes were consistently significantly bigger than BMP2 cmRNA lipoplexes (Figure 2A, $p \leq 0.002$). The possible changes on the lipoplex size over time was evaluated. No statistical differences were found for the lipoplexes size over a period of 7 days (Figure 2A, $p > 0.05$). Interestingly, a positive zeta potential of 16.3 ± 0.9 mV was found for MetLuc cmRNA, while a low, near zero 1.79 ± 1.6 mV was found for BMP2 cmRNA. Statistical significance was found when comparing the zeta potential of MetLuc cmRNA to that of BMP2 cmRNA (Figure 2A, $p \leq 0.0002$). Similar to the lipoplexes' size, the zeta potential did not show significant variation over time (Figure 2A, $p > 0.05$). However, for BMP2 cmRNA, the zeta potential became 0.08 ± 0.93 mV at day 5 and changed negative (−0.174 ± 1.37 mV) at day 7 after formulation.

MetLuc and BMP2 cmRNAs were efficiently incorporated into the lipidoid particles. Figure 2B shows a mean complexation efficiency of 92.6% for MetLuc and 95.6% for BMP2 cmRNA. The complexation efficiency slightly increased over time reaching values close to 100%. The integrity of MetLuc and BMP2 cmRNA was well preserved after complexation and over time. This can be concluded from Figure 2C, where RNA quality number (RQN) values of 9.6 and 10 were obtained for MetLuc cmRNA and BMP2 cmRNA, respectively. In addition, RQN values above 8 were obtained for all samples collected at different incubation times (up to 6 days post-complexation), indicating that little degradation occurred over days of incubation.

Biomaterial Coating of Ti Disks: Morphological Characterization. Ti disks' surface profile featured parallel polishing lines (Figure 3A,B right panel), and the sample was characterized by an average Sa of 0.25 μm (Figure 3D). PDLLA coating of the Ti disks slightly changed the surface profile. Figure 3 shows the SEM images, surface images, and surface profile of the highest and lowest concentrations of PDLLA used (*i.e.*, 3 and 0.25 mg/disk). To appreciate these results for all the PDLLA concentrations used, please see Figure S3 of the Supporting Information. By increasing the polymeric concentration, a rougher surface profile was obtained in which the polishing lines on the plain Ti disk were no longer observed (Figures 3A−C and S3A−C of the Supporting Information). This observation was confirmed by the quantification results of Sa and Ra (Figures 3D and S3D of the Supporting Information). The values of Sa and Ra for PDLLA 0.5 Ti disks and PDLLA 0.25 Ti disks were similar to those obtained for Ti disks (uncoated). A slight increase in the surface roughness parameters was observed for PDLLA 1 Ti, PDLLA 2 Ti, and PDLLA 3 Ti disks (Figures 3D and S3D of

https://dx.doi.org/10.1021/acs.molpharmaceut.0c01042
Mol. Pharmaceutics 2021, 18, 1121−1137

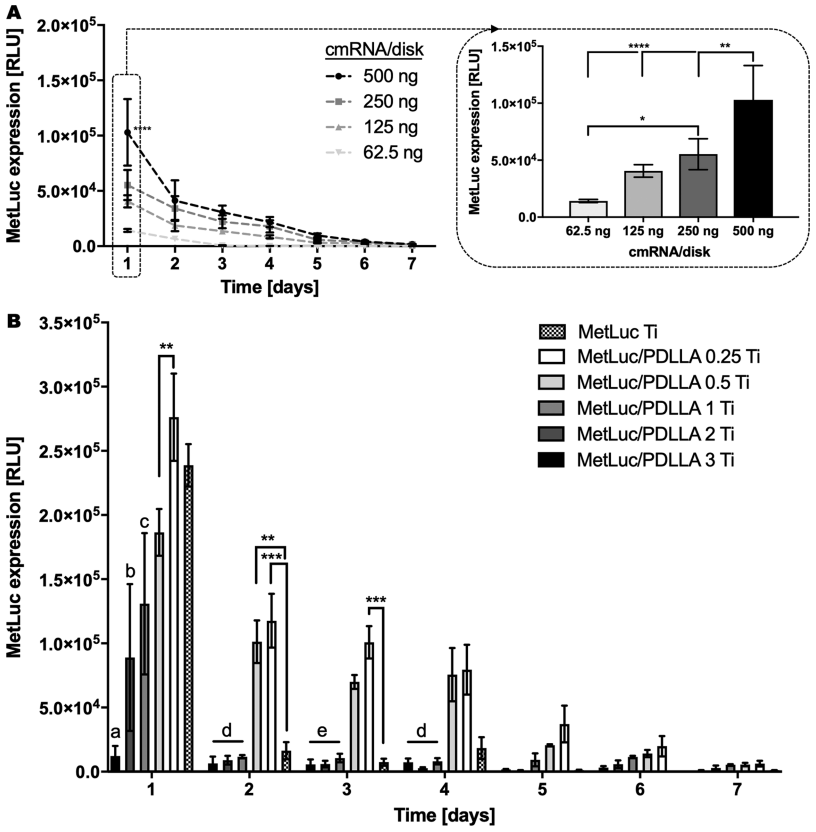

Figure 4. Transfection of NIH3T3 cells on MetLuc Ti and MetLuc PDLLA Ti disks. (A) MetLuc expression on Ti disks in which cmRNA was incorporated by means of physical adsorption. Different concentrations of cmRNA were used. The insert chart is a blow-up graph of day 1 after transfection showing the effect of different cmRNA concentrations used. **** indicates a significant decrease in expression after day 1 for the 500 ng cmRNA disk ($p < 0.0001$). Statistical significance on the insert chart is indicated by *$p = 0.0169$ (250 *vs* 62.5 ng), **$p = 0.0011$ (500 *vs* 250 ng), and ****$p < 0.0001$ (500 *vs* 125 ng and 500 *vs* 62.5 ng). (B) MetLuc expression obtained using MetLuc PDLLA Ti disks. MetLuc cmRNA was incorporated on Ti disks by means of physical adsorption with a subsequent deposition of a PDLLA protective layer. PDLLA concentrations varied from 0.25 up to 3 mg/disk. Statistical significance was indicated by ** ($p < 0.01$) and *** ($p < 0.001$). In addition, letters from *a* to *e* are used to indicate specific significance on each observation day. On day 1, *a* indicates a significantly lower expression for MetLuc/PDLLA 3 Ti when compared to all other groups ($p \leq 0.0109$); *b* indicates a significantly lower expression for MetLuc/PDLLA 2 Ti when compared to MetLuc/PDLLA 0.5 Ti, MetLuc/PDLLA 0.25 Ti, and MetLuc Ti disks ($p \leq 0.0005$); *c* indicates a significantly lower expression for MetLuc/PDLLA 1 Ti when compared to MetLuc/PDLLA 0.25 Ti and MetLuc Ti disks ($p \leq 0.0001$). On day 2, *d* indicates a significantly lower expression for MetLuc/PDLLA 3 Ti, MetLuc/PDLLA 2 Ti, and MetLuc/PDLLA 1 Ti when compared to MetLuc/PDLLA 0.5 Ti and MetLuc/PDLLA 0.25 Ti ($p \leq 0.001$). On day 3, *e* indicates a significantly lower expression for MetLuc/PDLLA 3 Ti, MetLuc/PDLLA 2 Ti, and MetLuc/PDLLA 1 Ti when compared to MetLuc/PDLLA 0.25 Ti ($p \leq 0.001$). Similar to day 2, on day 4, *d* indicates a significantly lower expression for MetLuc/PDLLA 3 Ti, MetLuc/PDLLA 2 Ti, and MetLuc/PDLLA 1 Ti when compared with MetLuc/PDLLA 0.5 Ti and MetLuc/PDLLA 0.25 Ti ($p \leq 0.03$). Two-way ANOVA, followed by Tukey's test was performed to analyze the data presented in (A,B). The results of statistical analysis are depicted in Tables S1 and S2 of the Supporting Information, respectively.

the Supporting Information). However, this increase of the surface roughness with higher PDLLA concentrations was statistically not significant. In contrast, the fibrin and fibrinogen coatings significantly impacted the surface roughness and the morphology of the coating. 1F0T Ti disks (fibrinogen) and 1F1T Ti disks (fibrin) showed substantially rougher surface profiles than those of PDLLA Ti disks and Ti disks (Figure 3A–C left panel). The values of Sa were significantly higher for the 1F0T Ti disk (fibrinogen) and 1F1T Ti disk (fibrin) samples when compared to those of PDLLA Ti disks (all concentrations) and Ti disks. Sa = 3.97 μm was obtained for 1F0T Ti disks (fibrinogen), while a value of 2.12 μm was obtained for 1F1T Ti disks (fibrin) (Figure 3D). Similarly, Ra was 4.21 μm for 1F0T Ti disks (fibrinogen) and 2.01 μm for 1F1T Ti disks (fibrin) (Figure S3D of the Supporting Information). Interestingly, although Sa and Ra values are noticeably higher for fibrinogen coatings, no statistical significance was found between those and the ones coated with fibrin.

Optimization of cmRNA Coating on Ti Disks: Physical Adsorption. Ti disks coated with MetLuc cmRNA lipoplexes were able to effectively transfect NIH3T3 cells (Figure 4A). The highest MetLuc expression levels were observed at 24 h after transfection for all cmRNA concentrations tested. Increasing the amount of cmRNA to 500 ng/disk resulted in a significant increase on MetLuc expression at 24 h post-transfection (blown-up insert in Figure 4A, $p = 0.0011$). Interestingly, a rapid decay of MetLuc expression was observed at 48 h post-transfection. By day 5 after transfection, MetLuc expression was negligible. No significant differences were found among the different cmRNA concentrations evaluated from day 2 post-transfection onward (Figure 4A, $p > 0.05$). A significant interaction between the cmRNA concentration and the expression over time was indicated by ANOVA (Table S1

https://dx.doi.org/10.1021/acs.molpharmaceut.0c01042
Mol. Pharmaceutics 2021, 18, 1121−1137

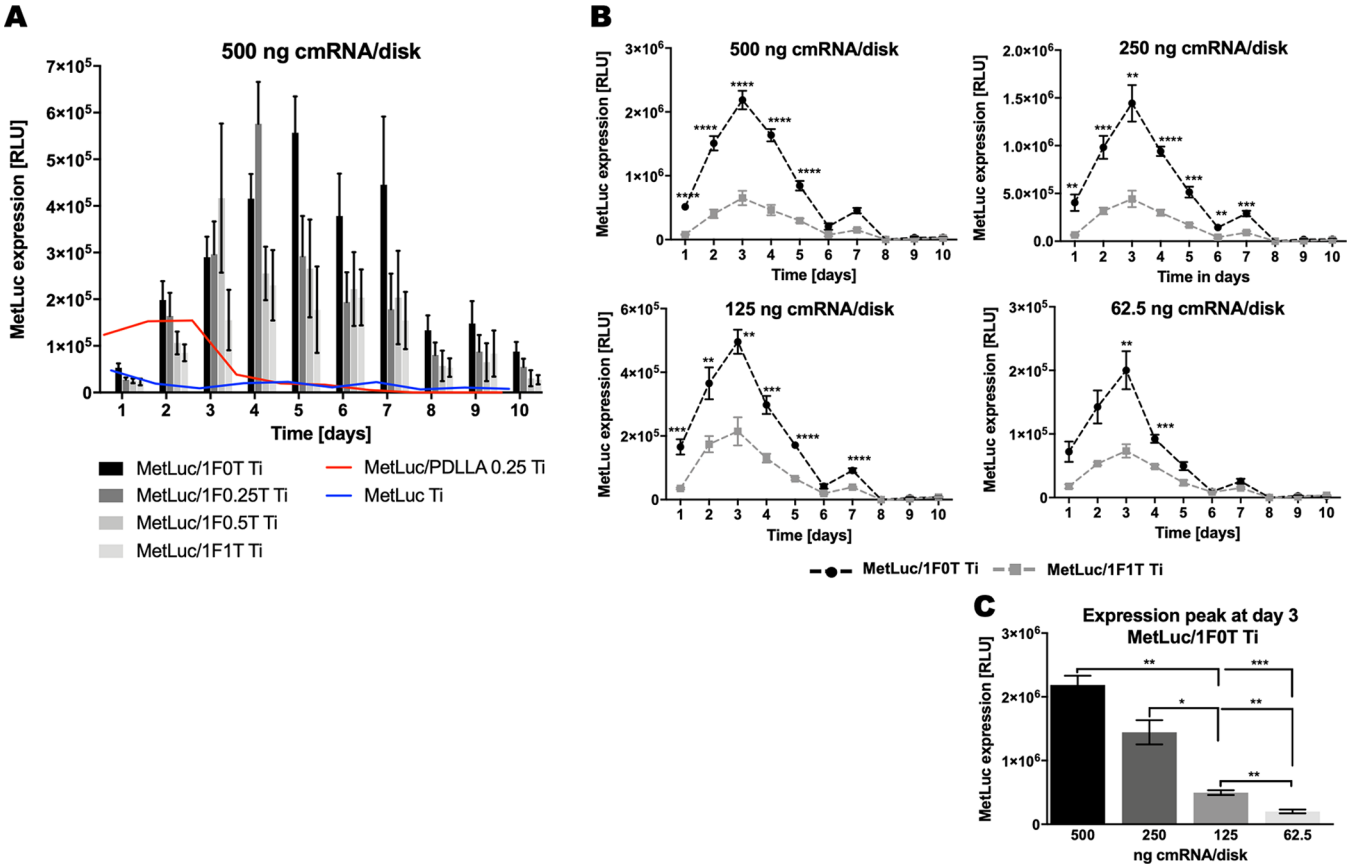

Figure 5. Transfection of NIH3T3 cells with MetLuc/1FZT Ti disks, where *Z* indicates different amounts of thrombin used. MetLuc Ti and MetLuc/PDLLA 0.25 Ti disks were used for comparison. (A) Comparison of MetLuc expression obtained over time using Ti disks in which 500 ng MetLuc cmRNA was incorporated by means of physical adsorption, physical adsorption with a subsequent deposition of a PDLLA protective layer, or physical entrapment. Two-way ANOVA, followed by Tukey's test was performed for data analysis. The results of statistical analysis are depicted in Table S3 of the Supporting Information. (B) Direct comparison between fibrin (MetLuc/1F1T) and fibrinogen (MetLuc/1F0T) coating in terms of MetLuc expression: effect of MetLuc cmRNA concentration incorporated into the coating. Multiple, unpaired *t*-test corrected for multiple comparisons by a Holm−Sidak method was performed for data analysis. (C) MetLuc expression at day 3 (expression peak) for the MetLuc/1F0T Ti disks with different amounts of cmRNA loaded into the coating. $*p \leq 0.05$, $**p \leq 0.01$, $***p \leq 0.001$, and $****p \leq 0.0001$. Repeated measures of one-way ANOVA, followed by Tukey's test were performed for data analysis.

of the Supporting Information). In fact, a different pattern of expression decay over time can be observed that is dependent on the cmRNA concentration used (Figure 4A).

Physical Adsorption with PDLLA Layer. The addition of a PDLLA protective layer to the MetLuc Ti disks prolonged the levels of MetLuc expression over a period of 7 days (Figure 4B). Interestingly, little effect was observed at 24 h post-transfection. At this time of observation, comparable expression levels were obtained for MetLuc Ti disks and for the best sample among the PDLLA Ti disks (*i.e.*, MetLuc/PDLLA 0.25 Ti disks) (p = 0.1850). Among the different PDLLA concentrations tested, the layer with the lowest polymeric concentration, that is, 0.25 mg/disk gave the best results. In fact, MetLuc expression was clearly dependent on the concentration of the PDLLA protective layer. The results indicated improved translation as the concentration of PDLLA in the coating decreased. A significant interaction between the PDLLA concentration and the expression over time was shown by ANOVA (Table S2 of the Supporting Information). Remarkably, from 48 h post-transfection onward, MetLuc/PDLLA 0.25 Ti and MetLuc/PDLLA 0.5 Ti resulted in higher MetLuc expression when compared to MetLuc Ti disks. Yet, this increase in expression was statistically significant only for 48 and 72 h post-transfection (MetLuc/PDLLA 0.25 Ti: p = 0.0002 for 48 h and p = 0.0009 for 72 h; MetLuc/PDLLA 0.5 Ti: p = 0.0034 for 48 h). PDLLA concentrations between 1 and 3 mg/disk resulted in negligible MetLuc expression at 48 h post-transfection and until the end of the experiment.

Physical Entrapment with Fibrin and Fibrinogen. Entrapment of MetLuc cmRNA lipoplexes inside fibrin and fibrinogen positively impacted MetLuc expression. The levels of expression were higher than those obtained for MetLuc Ti disks and for all formulations of MetLuc/PDLLA Ti disks (Figure 5A). This was statistically significant at 72 h post-transfection and onward (p < 0.05 for all comparisons). Remarkably, entrapment within a fibrin or fibrinogen network delayed the expression peak to 5 days post-transfection. As a reminder, this peak was observed at 24 h after transfection on MetLuc Ti disks and MetLuc/PDLLA Ti disks. Furthermore, a prolonged expression was observed when using fibrin or fibrinogen. At 7 days post-transfection, significant levels of MetLuc were detected in the supernatants for MetLuc/1F*X*T Ti disks (p < 0.0001). MetLuc expression was detectable for up to 10 days after transfection. Interestingly, fibrinogen coating resulted in the highest MetLuc expression for all times of observation analyzed, with the exception of 3- and 4-days post-

https://dx.doi.org/10.1021/acs.molpharmaceut.0c01042
Mol. Pharmaceutics 2021, 18, 1121−1137

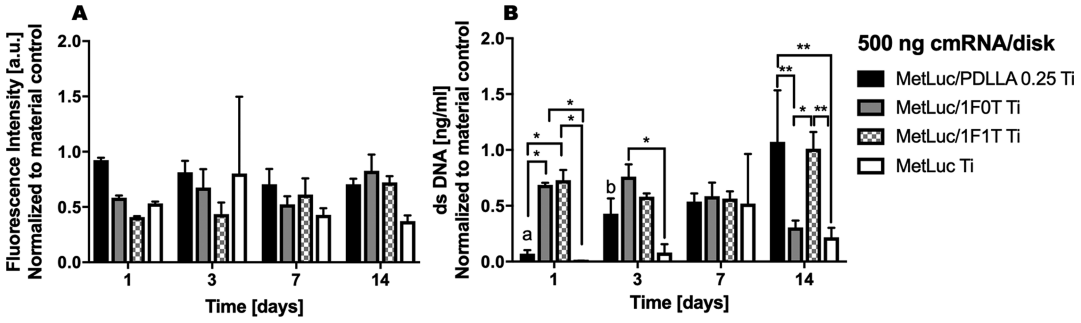

Figure 6. (A) Cell viability and (B) cell proliferation of NIH3T3 cells cultured on MetLuc Ti, MetLuc/PDLLA 0.25 Ti, MetLuc/1F1T Ti (fibrin), and MetLuc/1F0T Ti (fibrinogen) disks. The obtained results were normalized to material control, *i.e.*, uncoated titanium. The loaded cmRNA amount was 500 ng/disk. *$p \leq 0.05$; **$p \leq 0.01$. Two-way ANOVA, followed by Tukey's test was performed to analyze the data. The results of statistical analysis are depicted in Tables S4 and S5 of the Supporting Information.

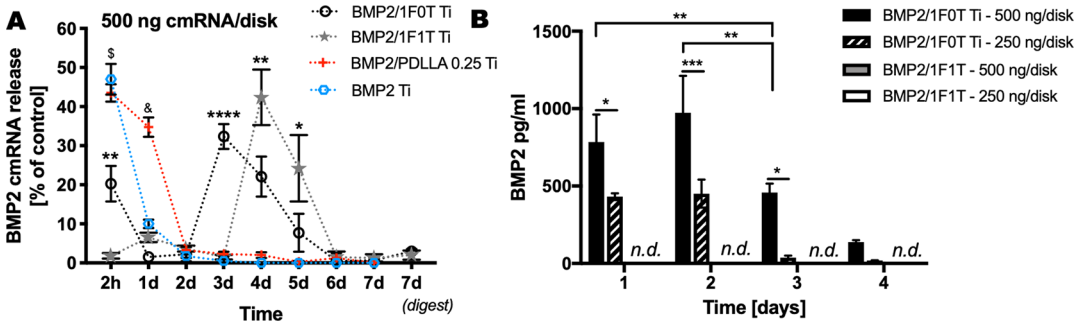

Figure 7. (A) BMP2 cmRNA release from BMP2 Ti, BMP2/PDLLA 0.25 Ti, BMP2/1F1T Ti (fibrin), and BMP2/1F0T Ti (fibrinogen) disks. The loaded BMP2 cmRNA amount was 500 ng/disk. For fibrin and fibrinogen coatings, the material was enzymatically digested after 7 days and the amount of cmRNA was assayed (digest). *$p \leq 0.05$, **$p \leq 0.01$, and ****$p \leq 0.0001$ comparing BMP2/1F1T Ti (fibrin) and BMP2/1F0T Ti (fibrinogen). At 2 h, $ (BMP2 Ti and BMP2/PDLLA 0.25 Ti) indicates p values < 0.0001 *vs* fibrin and fibrinogen. No differences were found between MetLuc Ti and MetLuc/PDLLA 0.25 Ti disks for this time of observation. At day 1, & (BMP2/PDLLA 0.25 Ti) indicates p values < 0.0001 compared to all studied groups. (B) BMP2 produced *in vitro* by C2C12 cells as a result of BMP2 cmRNA transfections on BMP2/1F1T Ti (fibrin) and BMP2/1F0T Ti (fibrinogen) disks. Two different cmRNA amounts were used, *i.e.*, 250 and 500 ng/disk. n.d. indicates not detected. *$p \leq 0.05$, **$p \leq 0.01$, and ***$p \leq 0.001$. Two-way ANOVA, followed by Tukey's test was performed to analyze the data. In the case of (A), a mixed-effect model (REML) was used. The results of statistical analysis are depicted in Tables S6 and S7 of the Supporting Information.

transfection. At those times of observation, MetLuc/1F0.5T Ti and MetLuc/1F0.25T Ti disks showed the highest MetLuc expression. The increase in MetLuc expression for the fibrinogen coating was significant when compared to all fibrin formulations at day 5 ($p < 0.01$) and day 7 ($p < 0.03$) post-transfection. In fact, lowering the thrombin concentration in the composition of the fibrin gel gradually increased the MetLuc expression.

Next, the effect of fibrin and fibrinogen coating on MetLuc expression was studied for different cmRNA concentrations (Figure 5B). The superiority of fibrinogen coating showed to be independent of the amount of cmRNA entrapped inside the network. As expected, MetLuc expression increased with increasing cmRNA concentrations (Figure 5C, $p < 0.05$).

Cell Viability and Proliferation of NIH3T3 Seeded on cmRNA Ti Disks, Uncoated and Coated with PDLLA, Fibrin, or Fibrinogen. Coating of MetLuc Ti disks with either PDLLA, fibrin, or fibrinogen seems to positively impact the cell viability. The alamarBlue results shown in Figure 6A indicated better cell viability for PDLLA-coated disks at 24 h after cell seeding. Nevertheless, an improved cell viability was observed for all coatings when compared to MetLuc Ti disks for later times of observation, that is, 14 days after seeding. Yet, no significant interaction was found by ANOVA between the type of coating and the cell viability over time (Table S4 of the Supporting Information). In contrast, a significant interaction was found for cell proliferation over time (Table S5 of the Supporting Information). In fact, a clearer effect of the disk coatings was observed in the cell proliferation ability (Figure 6B). Cell proliferation significantly increased in the fibrin- and fibrinogen-coated MetLuc disks ($p < 0.03$) although this effect was less noticeable over time. Interestingly, at day 14 of cell seeding, MetLuc/PDLLA 0.25 Ti and MetLuc 1F1T Ti (fibrin) disks resulted in significantly higher cell proliferation compared to the MetLuc Ti disks ($p = 0.0023$ for PDLLA and $p = 0.0048$ for fibrin).

BMP2 cmRNA-Activated Ti Disks. BMP2 cmRNA was quickly released from BMP2 Ti disks and BMP2/PDLLA 0.25 Ti disks (Figure 7A, $p < 0.0001$). BMP2 Ti disks showed a burst release of BMP2 cmRNA after 2 h that rapidly decayed after 1 day of incubation. At 2 days, minimal BMP2 cmRNA was detected. A similar BMP2 cmRNA release pattern was observed for BMP2/PDLLA 0.25 Ti disks. The burst release occurred up to 1 day ($p < 0.0001$) with subsequent full decline at 2 days post-incubation. In contrast, BMP2 cmRNA was released from BMP2/1F0T Ti and BMP2/1F1T Ti disks up to 6 days *in vitro* (Figure 7A). At day 7 post-transfection, negligible amounts of BMP2 cmRNA were found in either the supernatants or the cell lysates. The release profile showed a burst release of BMP2 cmRNA from BMP2/1F0T Ti as early as 2 h after incubation in media ($p = 0.0035$). Thereafter, both coatings showed similar release patterns. For BMP2/1F0T Ti,

https://dx.doi.org/10.1021/acs.molpharmaceut.0c01042
Mol. Pharmaceutics 2021, 18, 1121−1137

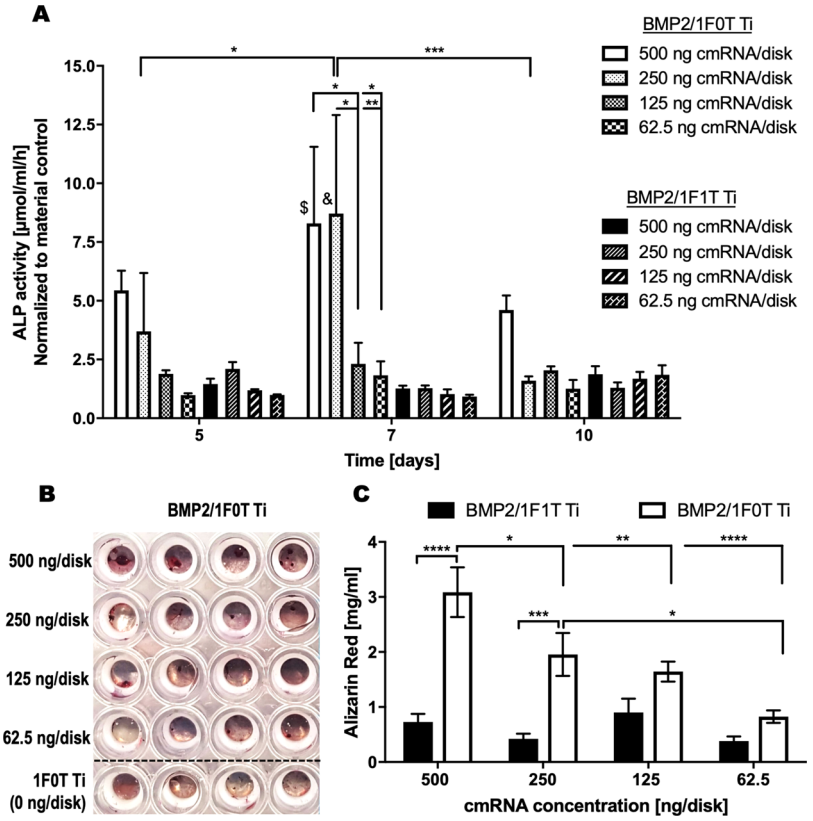

Figure 8. *In vitro* osteogenesis of C2C12 cells as a result of BMP2 cmRNA transfection using BMP2/1F1T Ti (fibrin) and BMP2/1F0T Ti (fibrinogen) disks. Different BMP2 cmRNA amounts were incorporated into the coatings, namely, 62.5 125, 250, and 500 ng/disk. (A) ALP activity determined at 5, 7, and 10 days after transfection. The obtained results were normalized to material control, *i.e.*, uncoated titanium. Statistical significance is indicated by $*p \leq 0.05$, $**p \leq 0.01$, and $***p \leq 0.001$. In addition, at day 7, $ indicates a p value of 0.0053 (500 ng cmRNA/disk in fibrin *vs* fibrinogen) and & indicates a p value of 0.0026 (250 ng cmRNA/disk in fibrin *vs* fibrinogen). (B) Alizarin Red staining in a representative plate corresponding to the BMP2/1F0T Ti (fibrinogen) disks. (C) Alizarin Red quantification at 35 days after transfection. $*p \leq 0.05$, $**p \leq 0.01$, $***p \leq 0.001$, and $****p \leq 0.0001$. Two-way ANOVA, followed by Tukey's test was performed to analyze the data presented in (A,C). The results of statistical analysis are depicted in Tables S8 and S9 of the Supporting Information, respectively.

a peak on BMP2 cmRNA release was observed at 3 days post-incubation while for BMP2/1F1T Ti disks this was detected at 4 days post-incubation. Thereafter, BMP2 cmRNA release from both coatings showed decay over time. In fact, no BMP2 cmRNA was detected in samples collected at days 10 or 14 post-release. Noteworthily, the area under the release curve was 78.75 for BMP2/1F0T Ti disks and 82.93 for BMP2/1F1T Ti disks.

BMP2/1F0T Ti (fibrinogen) disks and BMP2/1F1T Ti (fibrin) disks were used to evaluate the transfection efficiency of BMP2 cmRNA. BMP2 protein production was detected only in the C2C12 cell culture supernatants of the BMP2/1F0T Ti disks (Figure 7B). Interestingly, cells entrapped in the BMP2/1F1T coating did not produce detectable BMP2 proteins at any of the studied observation times (up to 4 days). For the two different amounts of BMP2 cmRNA loaded into the BMP2/1F0T Ti disks, that is, 500 and 250 ng/disk, the levels of produced BMP2 were significantly higher for 500 ng/disk (Figure 7B, $p < 0.03$). A significant interaction between the cmRNA concentration and the BMP2 expression over time was shown by ANOVA (Table S7 of the Supporting Information).

Osteoinduction. Besides the transfection capability, one important parameter for such osteoinductive transcript-activated matrix is its functionality. To test this, ALP activity and calcium deposition were evaluated post-transfection. An increase in ALP activity was detected in C2C12 cells entrapped within the BMP2/1F0T-coated Ti disks (Figure 8A).

The highest cmRNA concentrations used in those disks, that is, 500 and 250 ng/disk, significantly stimulated ALP activity of cells up to 7 days post-transfection ($p < 0.005$). At day 10, however, only the 500 ng/disk resulted in elevated ALP activity although not significant. No increase in ALP activity was detected in C2C12 cells transfected on BMP2/1F1T Ti disks (fibrin) for any time of observation. Here, no significant interaction was found by ANOVA between the sample group and the ALP activity over time (Table S8 of the Supporting Information). Similarly, Alizarin Red staining confirmed the formation of calcified nodules on the surface of BMP2/1F0T Ti disks (Figure 8B,C). Calcium deposits proportionally decreased with the cmRNA concentration used (Figure 8C). This decrease was found to be significant ($p < 0.018$) except for the direct comparison between the disks with 125 and 62.5 ng of cmRNA ($p = 0.12$). In fact, a significant interaction was found by ANOVA between the cmRNA concentration used and the concentration of Alizarin Red detected over time (Table S9 of the Supporting Information). Contrarily, negligible calcium deposition was detected for the BMP2/1F1T Ti disks (fibrin) (Figure 8C).

Neither ALP activity nor positive Alizarin Red staining was detected on uncoated Ti disks used as material control.

https://dx.doi.org/10.1021/acs.molpharmaceut.0c01042
Mol. Pharmaceutics 2021, 18, 1121−1137

DISCUSSION

Orthopedic metallic implant success is greatly reliant on integration with the surrounding bone. Loosening of the implant has been reported as one of the main causes of implant failure in orthopedics.[41] This is even more noticeable in patients who feature poor bone quality and quantity surrounding the implantable device. To avoid this, the ideal implant should be able to promote osteointegration and minimize infections. Biocompatibility and corrosion resistance are also desired features.[42] Much research has been conducted in terms of materials science to improve metallic implant biofeatures, having surface coating at the forefront. In this work, we describe the development of biocompatible and osteogenic BMP2 transcript-activated coatings to titanium surfaces.

Transcript therapy, that is, using mRNA to translate into therapeutic proteins, has recently been shown to be highly attractive for bone tissue healing.[27,35,43,44] We and others developed cmRNA coding for BMP2[27,34−36,43] and BMP9[45,46] that showed osteogenic potential *in vitro* and *in vivo*. In recent *in vivo* investigations, it has been demonstrated that when the BMP is synthesized endogenously, expression of BMP needs to be neither prolonged nor present in high concentrations for effective bone healing.[47] This makes transcript therapy particularly attractive for bone regeneration. However, the applicability of mRNA relies on eradicating its intrinsic immunogenicity and instability. This can be achieved by introducing modifications to the mRNA during the IVT production. In this study, we successfully produced cmRNAs by using chemically modified cytidine and uridine. We substituted up to 35% ribonucleotides with their modified analogues. Carlsson *et al.* reported that a full substitution of uridine with N1-methylpseudouridine in VEGF-A mRNA resulted in a nonimmunogenic and functional cmRNA.[48] Based on our previous findings, we also introduced a translation initiator of short 5′UTR (TISU) sequence and deleted an upstream open reading frame and an extra polyadenylation signal, followed by an adenylate−uridylate-rich region as part of the mRNA modifications to improve the translational efficiency.[35] By applying these modifications to mRNA in this study, we successfully obtained cmRNAs that encoded MetLuc and BMP2. Our results demonstrated high integrity and lack of degradation of MetLuc cmRNA and BMP2 cmRNA. Furthermore, both cmRNAs showed high transfection efficiency when administered to NIH3T3 and C2C12 cells. This is in agreement with our previous work[35,49] and the work of Kormann *et al.*[30] that show improved mRNA stability, and thus, translational efficiency after modifications have been done.

Once complexed with cationic lipidoid vectors, BMP2 cmRNA lipoplexes featured small size and also low zeta potential (<2 mV). Close to zero zeta potential may favor the agglomeration of lipoplexes. Therefore, we evaluated the stability of formed lipoplexes for up to 7 days. Interestingly, no agglomeration was detected and the dispersion remained homogeneous in size distribution (polydispersity index < 0.2). This coincides with our previous observations and with that of Li *et al.*[50] The authors obtained the highest luciferase expression for lipoplexes whose zeta potential was close to zero. They concluded that size, not surface charge, was the major determinant of lipofection efficiency. Additional stabilization of BMP2 cmRNA may have been provided by the cationic lipidoid used in our study to form the lipoplexes. These lipids provide moderate attachment to the negative backbone of the RNA, which helps to stabilize the complex.[51] Although the impact of lipoplex size on transfection efficiency is controversial (reviewed in ref 52), it has been reported that particles with a smaller size would gain high transfection efficiency.[53] Also, small particle size, that is, <80 nm has been reported as a requirement for high efficiency *in vivo* delivery.[52] This is a crucial feature for the translation of these complexes into the clinical arena.

To achieve our goal of incorporating BMP2 cmRNA lipoplexes onto the surface of Ti, we evaluated several surface functionalization methodologies. This evaluation was performed using a MetLuc (reporter) cmRNA. In our study, we decided to employ physical methods, that is, physical adsorption and physical entrapment. This is justified by the simplicity of these methodologies when compared with, for example, covalent binding that requires previous introduction of chemical functional groups on the surface of Ti. In addition, physical methods guarantee a lack of interference with the structure of the used biomolecules,[3] in our case with the cmRNA lipoplexes. The available literature supports our selection; physical methods have been utilized successfully in functionalizing the surface of Ti implants with biomolecules.[54−56] As expected, the incorporation of cmRNA lipoplexes *via* biomaterial coatings led to better results than directly depositing cmRNA complexes on Ti. In our study, we used PDLLA, fibrin, and fibrinogen as biomaterials for cmRNA surface incorporation. We speculate that the use of coatings made of these biomaterials may aid in protecting the cmRNA lipoplexes from the surrounding environmental factors, such as temperature and pH,[57] and from RNase degradation. Importantly, biomaterial coatings may also delay fast desorption and uncontrolled release of lipoplexes from the metallic surface. Our results confirmed this statement. BMP2 cmRNA was released significantly faster from uncoated Ti when compared to PDLLA-, fibrin-, or fibrinogen-coated Ti surfaces. This is in agreement with the observations of Jia and Kerr.[58] The authors reported an initial burst release of ibuprofen from titanium dioxide nanotubes that was followed by 90% release within the first hour of incubation. By coating the surface of titanium dioxide nanotubes with PLGA, the release was prolonged for up to 9 days. Bae *et al.* also observed a rapid release of BMP2 protein from titanium when no polymer coating was used.[59] In our study, coating with PDLLA still resulted in a fast cmRNA release characterized by an initial burst. Nevertheless, it did show a positive effect on the cmRNA transfection efficiency. It is worth mentioning that this positive effect could be maximized by adjusting the percentage of polymer in the coating. We observed an increase in cmRNA transfection in coatings with the lowest PDLLA concentration. This is in line with the reports of Kolk *et al.* using plasmid DNA.[12] The authors found higher gene-transfer efficiencies in titanium surfaces with the thinner PDLLA coating. Thinner coatings were obtained using the lowest PDLLA concentrations. Strobel *et al.*[60] and Sun *et al.*[61] described that titanium coated with low concentrations of PDLLA and PLGA, respectively, resulted in fast release of the entrapped drug. Based on these reports and our own results, we can postulate that polymeric coatings featuring low polymer concentrations may allow for a faster release of vector, thereby increasing the cellular uptake and transfection. Interestingly, in our study, coating of titanium with fibrin and fibrinogen resulted in more efficiency than that of PDLLA in terms of transfection

https://dx.doi.org/10.1021/acs.molpharmaceut.0c01042
Mol. Pharmaceutics 2021, 18, 1121−1137

efficiency. To establish a direct comparison between these coating materials is difficult because the physical entrapment strategy used was different for each case. We could not find any report directly comparing these materials for coating metallic surfaces. They all may be an appealing choice depending on the specific application of the coated implant. In the case of fibrin and fibrinogen, they form a 3D fibrous network that allow drug entrapment and cell colonization. These features are very much desired for a gene-transfer matrix. Surprisingly, fibrinogen coating resulted in a slightly faster release of BMP2 cmRNA than fibrin. It also supported higher transfection efficiencies and prolonged production of BMP2 protein by transfected cells. Jeon *et al.* observed that by increasing thrombin in the composition of fibrin, the release rate of entrapped drugs decreased.[62] One explanation for this observation may be based on the structure of the 3D network. Gels formed at low concentrations of thrombin or no thrombin at all (*i.e.*, fibrinogen) feature thin fibrils.[63] Also, as the concentration of thrombin decreases in fibrin gels, less dense cross-linked gels are formed.[62] This may result in a faster diffusion of entrapped molecules. In addition to that, the fibrinogen structure that can be formed without thrombin[64] has excellent adsorption on titanium surfaces.[65] This might lead to a more stable coating than fibrin. Another important point to consider is the biocompatibility and cell-attractant properties of fibrinogen. Fibrinogen is known to promote cell attachment and proliferation.[66] It has also been reported to stimulate cell infiltration into 3D scaffolds.[67] These cellular features of fibrinogen may have increased the cellular attachment to the fibrinogen-coated titanium, thereby increasing the transfection efficiency. In fact, all three coatings enhanced cell viability and proliferation when compared to the uncoated titanium surface. Cells may have been stimulated to attach to and colonize the coating by the highly biocompatible materials used in this study. On the other hand, biomaterial coatings prevent cells to be exposed to high doses of cmRNA lipoplexes in short time. Such fast exposure to high concentrations of lipoplexes may lead to increased toxicity. In fact, it has been reported that plasmid DNA complexes loaded into 3D matrices show reduced toxicity.[68,69] In these matrices, due to the co-localization of cells and lipoplexes, exposure to plasmid DNA complexes is rather gradual. Identically, in our study, cmRNA lipoplexes are not delivered at once into the cells but in a sustained fashion from the transcript-activated coatings deposited onto the titanium surfaces.

Cells transfected using the BMP2 cmRNA/fibrinogen-coated Ti (*i.e.*, BMP2/1F0T Ti disks) were able to secrete BMP2 *in vitro* that resulted in subsequent osteogenic differentiation. ALP activity increased and mineralization was also observed to be dependent on the cmRNA amount present on the coating. These results corroborate our previous published data in which osteogenesis strongly depends on the cmRNA dose used.[27,35] This holds true both *in vitro* and *in vivo*. From our published data, we have established 20 pg of BMP2 cmRNA/cell (human mesenchymal stem cell monolayers) to be osteogenic *in vitro*.[27] In this work, 50 pg of BMP2 cmRNA/cell was necessary to induce ALP activity and mineralization. It is worth mentioning that here a 3D coating was developed (instead of the cell monolayers used previously). Also, different cell types were used in both studies. *In vivo*, BMP2 cmRNA amounts higher than 5 μg seems to be necessary to heal a 5 mm critical bone defect in rats.[35] The optimal cmRNA dose for enhancing *in vivo* osteointegration of Ti implants using our titanium-activated matrices will be the subject of future research. Nevertheless, we estimate that 23 μg of BMP2 cmRNA would be necessary to coat 80% of the MiniHip (Corin Group, UK) stem in order to successfully achieve osteointegration in a patient. This estimation was performed for MiniHip hip prosthesis size 3 (length = 89 mm and media-to-lateral diameter = 25.8 mm), which is commonly used in patients.[70] Considering that >5 μg of BMP2 cmRNA seems to be necessary to treat a rat 5 mm non-union bone defect,[35] 23 μg of cmRNA per human hip prosthesis stem appears to be a feasible amount that grants affordability to this newly developed treatment. Moreover, 23 μg of cmRNA can be easily produced at low cost. The expected costs for producing GMP-grade cmRNA for clinical use are reported to be up to 10-folds lower than its recombinant protein counterpart.[71] Yet, to fully assess the feasibility of these newly developed implants, their *in vivo* biomechanical performance should be evaluated. Limitations of our work include lack of these biomechanical studies. The available literature demonstrated improvement on the biomechanical performance for fibrinogen- or PLGA-coated Ti screws[72,73] as well as for PDLLA Ti surfaces[74] after *in vivo* implantation. Remarkably, the authors showed tight integration of the material coatings to the Ti surfaces. This allowed the conclusion of the high adhesion features of the coatings to the metallic surfaces, regardless of the *in vivo* implantation methodology used.

To the best of our knowledge, cmRNA transcript-activated metallic implants have not been reported before. One study from Wu *et al.* reported microRNA-functionalized titanium surfaces by using mimics (miR-29b) and antagomirs (miR-138).[75] In a more recent study, Liu *et al.* incorporated antagomir (miR-204)−gold nanoparticles into a PLGA coating on titanium surfaces.[73] Both studies showed improved *in vitro* osteogenesis. Our work along with these two studies pioneers in demonstrating the potentiality that RNA therapeutics can bring to the field of metallic implants' osteointegration for dentistry and orthopedic applications.

CONCLUSIONS

We have investigated different methods for coating cmRNA on titanium surfaces. We found that metallic coating using biomaterials greatly improve the outcome of cmRNA transfer as well as cellular responses. Fibrinogen stands out as an optimal material for the coating of titanium. Our results supported that fibrinogen coating provided sustained delivery of loaded cmRNA lipoplexes, increased the transfection efficiency and attracted cells to the coating layer, and thereby improved the overall outcome. BMP2 cmRNA loaded onto fibrinogen-coated titanium disks induced ALP activity and mineralization of C2C12 cells *in vitro*, both indicators of successful osteogenic differentiation.

Overall, our findings support the use of fibrinogen as a biomaterial for loading RNA therapeutics to be used on metallic implant surfaces. Particularly, in the areas of ortho-regeneration, this biomaterial−nucleic acid combination allows obtaining transcript-activated matrices with outstanding features.

https://dx.doi.org/10.1021/acs.molpharmaceut.0c01042
Mol. Pharmaceutics 2021, 18, 1121−1137

■ ASSOCIATED CONTENT

Supporting Information

The Supporting Information is available free of charge at https://pubs.acs.org/doi/10.1021/acs.molpharmaceut.0c01042.

Protocol used to transfect NIH3T3 cells with produced MetLuc cmRNA and BMP2 cmRNA using Lipofectamine 2000, fragment analysis of produced cmRNAs, quality control of produced cmRNAs, MetLuc and BMP-2 expressions of NIH3T3 cells, morphological characterization of PDLLA coating of Ti disks with varying concentrations of PDLLA, quantification of arithmetic mean heights over line (Ra) for all studied Ti disks, and two-way ANOVA results (PDF)

■ AUTHOR INFORMATION

Corresponding Author

Elizabeth R. Balmayor − *IBE, MERLN Institute for Technology-Inspired Regenerative Medicine, Maastricht University, 6200 MD Maastricht, The Netherlands; Rehabilitation Medicine Research Center, Mayo Clinic, Rochester, Minnesota 55905, United States;* orcid.org/0000-0002-0484-4847; Phone: +31 6 27 07 16 78; Email: e.rosadobalmayor@maastrichtuniversity.nl

Authors

Omnia Fayed − *Institute of Molecular Immunology and Experimental Oncology-Klinikum Rechts der Isar, Technical University of Munich, 81675 Munich, Germany; Ethris GmbH, 82152 Planegg, Germany*

Martijn van Griensven − *cBITE, MERLN Institute for Technology-Inspired Regenerative Medicine, Maastricht University, 6200 MD Maastricht, The Netherlands; Rehabilitation Medicine Research Center, Mayo Clinic, Rochester, Minnesota 55905, United States;* orcid.org/0000-0001-5104-9881

Zeinab Tahmasebi Birgani − *IBE, MERLN Institute for Technology-Inspired Regenerative Medicine, Maastricht University, 6200 MD Maastricht, The Netherlands*

Christian Plank − *Institute of Molecular Immunology and Experimental Oncology-Klinikum Rechts der Isar, Technical University of Munich, 81675 Munich, Germany; Ethris GmbH, 82152 Planegg, Germany*

Complete contact information is available at: https://pubs.acs.org/10.1021/acs.molpharmaceut.0c01042

Notes

The authors declare no competing financial interest.
O.F. and C.P. are the employees of Ethris GmbH. C.P. is a shareholder of Ethris GmbH.

■ ACKNOWLEDGMENTS

O.F. is a recipient of a Ph.D. scholarship under the German−Egyptian Research Long-term Scholarship Program (GERLS) from the German Academic Exchange Service (DAAD) and the Egyptian Ministry of Higher Education Personal Funding Scheme. The authors acknowledge the support from Jan Lang and Peter Foehr in 3D printing of the Teflon inserts and Johannes Geiger during cmRNA production. The authors would also like to thank the experimental trauma surgery team for the assistance rendered during part of the cell culture experiments described here and for the utilization of the FLUOStar Omega plate reader equipment. The authors acknowledge the valuable help provided by Tristan Bodet and Denis van Beurden at MERLN for surface and morphological characterization of Ti disks.

■ REFERENCES

(1) Markatos, K.; Tsoucalas, G.; Sgantzos, M. Hallmarks in the history of orthopaedic implants for trauma and joint replacement. *Acta Medico-Historica Adriat.* **2016**, *14*, 161−176.

(2) Wang, W.; Poh, C. K. Titanium Alloys in Orthopaedics. In *Titanium Alloys: Advances in Properties Control*; Sieniawski, J., Ziaja, W., Eds.; IntechOpen, 2013.

(3) de Jonge, L. T.; Leeuwenburgh, S. C. G.; Wolke, J. G. C.; Jansen, J. A. Organic-inorganic surface modifications for titanium implant surfaces. *Pharm. Res.* **2008**, *25*, 2357−2369.

(4) Faensen, B.; Wildemann, B.; Hain, C.; Hohne, J.; Funke, Y.; Plank, C.; Stemberger, A.; Schmidmaier, G. Local application of BMP-2 specific plasmids in fibrin glue does not promote implant fixation. *BMC Musculoskeletal Disord.* **2011**, *12*, 163.

(5) Wang, J.; Guo, J.; Liu, J.; Wei, L.; Wu, G. BMP-functionalised coatings to promote osteogenesis for orthopaedic implants. *Int. J. Mol. Sci.* **2014**, *15*, 10150−10168.

(6) Noori, A.; Ashrafi, S. J.; Vaez-Ghaemi, R.; Hatamian-Zaremi, A.; Webster, T. J. A review of fibrin and fibrin composites for bone tissue engineering. *Int. J. Nanomed.* **2017**, *12*, 4937−4961.

(7) Prakasam, M.; Locs, J.; Salma-Ancane, K.; Loca, D.; Largeteau, A.; Berzina-Cimdina, L. Biodegradable Materials and Metallic Implants—A Review. *J. Funct. Biomater.* **2017**, *8*, 44.

(8) Smith, J. R.; Lamprou, D. A. Polymer coatings for biomedical applications: a review. *Trans. IMF* **2014**, *92*, 9−19.

(9) Auras, R.; Lim, L.-T.; Selke, S. E. M.; Tsuji, H. *Poly(Lactic Acid): Synthesis, Structures, Properties, Processing, and Applications*; John Wiley & Sons, Inc., 2010.

(10) Bettinger, T.; Carlisle, R. C.; Read, M. L.; Ogris, M.; Seymour, L. W. Peptide-mediated RNA delivery: a novel approach for enhanced transfection of primary and post-mitotic cells. *Nucleic Acids Res.* **2001**, *29*, 3882−3891.

(11) Fuchs, T. F.; Surke, C.; Stange, R.; Quandte, S.; Wildemann, B.; Raschke, M. J.; Schmidmaier, G. Local delivery of growth factors using coated suture material. *Sci. World J.* **2012**, *2012*, 109216.

(12) Kolk, A.; Haczek, C.; Koch, C.; Vogt, S.; Kullmer, M.; Pautke, C.; Deppe, H.; Plank, C. A strategy to establish a gene-activated matrix on titanium using gene vectors protected in a polylactide coating. *Biomaterials* **2011**, *32*, 6850−6859.

(13) Guo, Y.; Guan, J.; Peng, H.; Shu, X.; Chen, L.; Guo, H. Tightly adhered silk fibroin coatings on Ti6Al4V biometals for improved wettability and compatible mechanical properties. *Mater. Des.* **2019**, *175*, 107825.

(14) Sartori, M.; Giavaresi, G.; Parrilli, A.; Ferrari, A.; Aldini, N. N.; Morra, M.; Cassinelli, C.; Bollati, D.; Fini, M. Collagen type I coating stimulates bone regeneration and osteointegration of titanium implants in the osteopenic rat. *Int. Orthop.* **2015**, *39*, 2041−2052.

(15) van der Stok, J.; Koolen, M. K. E.; de Maat, M. P. M.; Yavari, S. A.; Alblas, J.; Patka, P.; Verhaar, J. A. N.; van Lieshout, E. M. M.; Zadpoor, A. A.; Weinans, H.; Jahr, H. Full regeneration of segmental bone defects using porous titanium implants loaded with BMP-2 containing fibrin gels. *Eur. Cells Mater.* **2015**, *29*, 141−154.

(16) Van Vlierberghe, S.; Vanderleyden, E.; Boterberg, V.; Dubruel, P. Gelatin functionalization of biomaterial surfaces: Strategies for immobilization and visualization. *Polymers* **2011**, *3*, 114−130.

(17) Ahmed, T. A. E.; Dare, E. V.; Hincke, M. Fibrin: a versatile scaffold for tissue engineering applications. *Tissue Eng., Part B* **2008**, *14*, 199−215.

(18) Laurens, N.; Koolwijk, P.; de Maat, M. P. M. Fibrin structure and wound healing. *J. Thromb. Haemostasis* **2006**, *4*, 932−939.

(19) Balmayor, E. R. Targeted delivery as key for the success of small osteoinductive molecules. *Adv. Drug Delivery Rev.* **2015**, *94*, 13−27.

(20) Mas-Moruno, C. Surface functionalization of biomaterials for bone tissue regeneration and repair. In *Peptides and Proteins as Biomaterials for Tissue Regeneration and Repair*; Barbosa, M. A., Martins, C. L., Eds.; WP Woodhead Publishing, Elsevier, 2018; pp 73−100.
(21) Schliephake, H.; Rublack, J.; Aeckerle, N.; Forster, A.; Schwenzer, B.; Reichert, J.; Scharnweber, D. In vivo effect of immobilisation of bone morphogenic protein 2 on titanium implants through nano-anchored oligonucleotides. *Eur. Cells Mater.* **2015**, *30*, 28−40.
(22) Fischer, J.; Kolk, A.; Wolfart, S.; Pautke, C.; Warnke, P. H.; Plank, C.; Smeets, R. Future of local bone regeneration - Protein versus gene therapy. *J. Cranio-Maxillofacial Surg.* **2011**, *39*, 54−64.
(23) Balmayor, E. R.; Feichtinger, G. A.; Azevedo, H. S.; van Griensven, M.; Reis, R. L. Starch-poly-ε-caprolactone Microparticles Reduce the Needed Amount of BMP-2. *Clin. Orthop. Relat. Res.* **2009**, *467*, 3138−3148.
(24) Ben-David, D.; Srouji, S.; Shapira-Schweitzer, K.; Kossover, O.; Ivanir, E.; Kuhn, G.; Müller, R.; Seliktar, D.; Livne, E. Low dose BMP-2 treatment for bone repair using a PEGylated fibrinogen hydrogel matrix. *Biomaterials* **2013**, *34*, 2902−2910.
(25) Bessa, P. C.; Balmayor, E. R.; Azevedo, H. S.; Nürnberger, S.; Casal, M.; van Griensven, M.; Reis, R. L.; Redl, H. Silk fibroin microparticles as carriers for delivery of human recombinant BMPs. Physical characterization and drug release. *J. Tissue Eng. Regener. Med.* **2010**, *4*, 349−355.
(26) Balmayor, E. R.; van Griensven, M. Gene therapy for bone engineering. *Front. Bioeng. Biotechnol.* **2015**, *3*, 9.
(27) Balmayor, E. R.; Geiger, J. P.; Aneja, M. K.; Berezhanskyy, T.; Utzinger, M.; Mykhaylyk, O.; Rudolph, C.; Plank, C. Chemically modified RNA induces osteogenesis of stem cells and human tissue explants as well as accelerates bone healing in rats. *Biomaterials* **2016**, *87*, 131−146.
(28) Evans, C.; De la Vega, R. E.; Evans, C. H.; van Griensven, M.; Balmayor, E. R. Healing with RNA. *Injury* **2019**, *50*, 625−626.
(29) Yamamoto, A.; Kormann, M.; Rosenecker, J.; Rudolph, C. Current prospects for mRNA gene delivery. *Eur. J. Pharm. Biopharm.* **2009**, *71*, 484−489.
(30) Kormann, M. S. D.; Hasenpusch, G.; Aneja, M. K.; Nica, G.; Flemmer, A. W.; Herber-Jonat, S.; Huppmann, M.; Mays, L. E.; Illenyi, M.; Schams, A.; Griese, M.; Bittmann, I.; Handgretinger, R.; Hartl, D.; Rosenecker, J.; Rudolph, C. Expression of therapeutic proteins after delivery of chemically modified mRNA in mice. *Nat. Biotechnol.* **2011**, *29*, 154−157.
(31) Jarzębińska, A.; Pasewald, T.; Lambrecht, J.; Mykhaylyk, O.; Kümmerling, L.; Beck, P.; Hasenpusch, G.; Rudolph, C.; Plank, C.; Dohmen, C. A Single Methylene Group in Oligoalkylamine-Based Cationic Polymers and Lipids Promotes Enhanced mRNA Delivery. *Angew. Chem., Int. Ed. Engl.* **2016**, *55*, 9591−9595.
(32) Malone, R. W.; Felgner, P. L.; Verma, I. M. Cationic liposome-mediated RNA transfection. *Proc. Natl. Acad. Sci. U.S.A.* **1989**, *86*, 6077−6081.
(33) Rejman, J.; Tavernier, G.; Bavarsad, N.; Demeester, J.; De Smedt, S. C. mRNA transfection of cervical carcinoma and mesenchymal stem cells mediated by cationic carriers. *J. Controlled Release* **2010**, *147*, 385−391.
(34) Balmayor, E. R.; Geiger, J. P.; Koch, C.; Aneja, M. K.; van Griensven, M.; Rudolph, C.; Plank, C. Modified mRNA for BMP-2 in Combination with Biomaterials Serves as a Transcript-Activated Matrix for Effectively Inducing Osteogenic Pathways in Stem Cells. *Stem Cells Dev.* **2017**, *26*, 25−34.
(35) Zhang, W.; De La Vega, R. E.; Coenen, M. J.; Müller, S. A.; Peniche Silva, C. J.; Aneja, M. K.; Plank, C.; van Griensven, M.; Evans, C. H.; Balmayor, E. R. An Improved, Chemically Modified RNA Encoding BMP-2 Enhances Osteogenesis In Vitro and In Vivo. *Tissue Eng., Part A* **2019**, *25*, 131−144.
(36) Badieyan, Z. S.; Berezhanskyy, T.; Utzinger, M.; Aneja, M. K.; Emrich, D.; Erben, R.; Schüler, C.; Altpeter, P.; Ferizi, M.; Hasenpusch, G.; Rudolph, C.; Plank, C. Transcript-activated collagen matrix as sustained mRNA delivery system for bone regeneration. *J. Controlled Release* **2016**, *239*, 137−148.
(37) Jesorka, A.; Orwar, O. Liposomes: technologies and analytical applications. *Annu. Rev. Anal. Chem.* **2008**, *1*, 801−832.
(38) Kim, I. S.; Song, Y. M.; Cho, T. H.; Kim, J. Y.; Weber, F. E.; Hwang, S. J. Synergistic action of static stretching and BMP-2 stimulation in the osteoblast differentiation of C2C12 myoblasts. *J. Biomech.* **2009**, *42*, 2721−2727.
(39) Langenbach, F.; Handschel, J. Effects of dexamethasone, ascorbic acid and beta-glycerophosphate on the osteogenic differentiation of stem cells in vitro. *Stem Cell Res. Ther.* **2013**, *4*, 117.
(40) Katagiri, T.; Yamaguchi, A.; Komaki, M.; Abe, E.; Takahashi, N.; Ikeda, T.; Rosen, V.; Wozney, J. M.; Fujisawa-Sehara, A.; Suda, T. Bone morphogenetic protein-2 converts the differentiation pathway of C2C12 myoblasts into the osteoblast lineage. *J. Cell Biol.* **1994**, *127*, 1755−1766.
(41) Palmquist, A.; Thomsen, P.; Brånemark, R.; Engqvist, H.; Lausmaa, J. Retrieval and analysis of orthopaedic implants. In *Bone Repair Biomaterials*; Planell, J. A., Best, S. M., Lacroix, D., Merolli, A., Eds.; Woodhead Publishing, 2009; pp 423−440.
(42) Katti, K. S.; Verma, D.; Katti, D. R. Materials for joint replacement. In *Joint Replacement Technology*; Revell, P. A., Ed.; Woodhead Publishing, 2008; pp 81−104.
(43) Elangovan, S.; Khorsand, B.; Do, A.-V.; Hong, L.; Dewerth, A.; Kormann, M.; Ross, R. D.; Rick Sumner, D.; Allamargot, C.; Salem, A. K. Chemically modified RNA activated matrices enhance bone regeneration. *J. Controlled Release* **2015**, *218*, 22−28.
(44) Elangovan, S.; Kormann, M. S.; Khorsand, B.; Salem, A. K. The oral and craniofacial relevance of chemically modified RNA therapeutics. *Discov. Med.* **2016**, *21*, 35−39.
(45) Khorsand, B.; Elangovan, S.; Hong, L.; Dewerth, A.; Kormann, M. S. D.; Salem, A. K. A Comparative Study of the Bone Regenerative Effect of Chemically Modified RNA Encoding BMP-2 or BMP-9. *AAPS J.* **2017**, *19*, 438−446.
(46) Khorsand, B.; Elangovan, S.; Hong, L.; Kormann, M. S. D.; Salem, A. K. A bioactive collagen membrane that enhances bone regeneration. *J. Biomed. Mater. Res., Part B* **2019**, *107*, 1824−1832.
(47) Liu, F.; Ferreira, E.; Porter, R. M.; Glatt, V.; Schinhan, M.; Shen, Z.; Randolph, M. A.; Kirker-Head, C. A.; Wehling, C.; Vrahas, M. S.; Evans, C. H.; Wells, J. W. Rapid and reliable healing of critical size bone defects with genetically modified sheep muscle. *Eur. Cells Mater.* **2015**, *30*, 118−131.
(48) Carlsson, L.; Clarke, J. C.; Yen, C.; Gregoire, F.; Albery, T.; Billger, M.; Egnell, A.-C.; Gan, L.-M.; Jennbacken, K.; Johansson, E.; Linhardt, G.; Martinsson, S.; Sadiq, M. W.; Witman, N.; Wang, Q.-D.; Chen, C.-H.; Wang, Y.-P.; Lin, S.; Ticho, B.; Hsieh, P. C. H.; Chien, K. R.; Fritsche-Danielson, R. Biocompatible, Purified VEGF-A mRNA Improves Cardiac Function after Intracardiac Injection 1 Week Post-myocardial Infarction in Swine. *Mol. Ther.–Methods Clin. Dev.* **2018**, *9*, 330−346.
(49) Trepotec, Z.; Aneja, M. K.; Geiger, J.; Hasenpusch, G.; Plank, C.; Rudolph, C. Maximizing the Translational Yield of mRNA Therapeutics by Minimizing 5′-UTRs. *Tissue Eng., Part A* **2019**, *25*, 69−79.
(50) Li, W.; Ishida, T.; Okada, Y.; Oku, N.; Kiwada, H. Increased gene expression by cationic liposomes (TFL-3) in lung metastases following intravenous injection. *Biol. Pharm. Bull.* **2005**, *28*, 701−706.
(51) Zou, S.; Scarfo, K.; Nantz, M. H.; Hecker, J. G. Lipid-mediated delivery of RNA is more efficient than delivery of DNA in non-dividing cells. *Int. J. Pharm.* **2010**, *389*, 232−243.
(52) Ma, B.; Zhang, S.; Jiang, H.; Zhao, B.; Lv, H. Lipoplex morphologies and their influences on transfection efficiency in gene delivery. *J. Controlled Release* **2007**, *123*, 184−194.
(53) Kneuer, C.; Ehrhardt, C.; Bakowsky, H.; Ravi Kumar, M. N. V.; Oberle, V.; Lehr, C. M.; Hoekstra, D.; Bakowsky, U. The influence of physicochemical parameters on the efficacy of non-viral DNA transfection complexes: a comparative study. *J. Nanosci. Nanotechnol.* **2006**, *6*, 2776−2782.

https://dx.doi.org/10.1021/acs.molpharmaceut.0c01042
Mol. Pharmaceutics 2021, 18, 1121−1137

(54) Civantos, A.; Martínez-Campos, E.; Ramos, V.; Elvira, C.; Gallardo, A.; Abarrategi, A. Titanium Coatings and Surface Modifications: Toward Clinically Useful Bioactive Implants. *ACS Biomater. Sci. Eng.* **2017**, *3*, 1245−1261.
(55) Gulati, K.; Kogawa, M.; Prideaux, M.; Findlay, D. M.; Atkins, G. J.; Losic, D. Drug-releasing nano-engineered titanium implants: therapeutic efficacy in 3D cell culture model, controlled release and stability. *Mater. Sci. Eng., C* **2016**, *69*, 831−840.
(56) Ren, L.; Pan, S.; Li, H.; Li, Y.; He, L.; Zhang, S.; Che, J.; Niu, Y. Effects of aspirin-loaded graphene oxide coating of a titanium surface on proliferation and osteogenic differentiation of MC3T3-E1 cells. *Sci. Rep.* **2018**, *8*, 15143.
(57) Chen, C.; Zhang, S.-M.; Lee, I.-S. Immobilizing bioactive molecules onto titanium implants to improve osseointegration. *Surf. Coat. Technol.* **2013**, *228*, S312−S317.
(58) Jia, H.; Kerr, L. L. Sustained ibuprofen release using composite poly(lactic-co-glycolic acid)/titanium dioxide nanotubes from Ti implant surface. *J. Pharm. Sci.* **2013**, *102*, 2341−2348.
(59) Bae, I.-H.; Yun, K.-D.; Kim, H.-S.; Jeong, B.-C.; Lim, H.-P.; Park, S.-W.; Lee, K.-M.; Lim, Y.-C.; Lee, K.-K.; Yang, Y.; Koh, J.-T. Anodic oxidized nanotubular titanium implants enhance bone morphogenetic protein-2 delivery. *J. Biomed. Mater. Res., Part B* **2010**, *93*, 484−491.
(60) Strobel, C.; Schmidmaier, G.; Wildemann, B. Changing the release kinetics of gentamicin from poly(D,L-lactide) implant coatings using only one polymer. *Int. J. Artif. Organs* **2011**, *34*, 304−316.
(61) Sun, S.; Zhang, Y.; Zeng, D.; Zhang, S.; Zhang, F.; Yu, W. PLGA film/Titanium nanotubes as a sustained growth factor releasing system for dental implants. *J. Mater. Sci.: Mater. Med.* **2018**, *29*, 141.
(62) Jeon, O.; Ryu, S. H.; Chung, J. H.; Kim, B. S. Control of basic fibroblast growth factor release from fibrin gel with heparin and concentrations of fibrinogen and thrombin. *J. Controlled Release* **2005**, *105*, 249−259.
(63) Ahmad, E.; Fatima, M. T.; Hoque, M.; Owais, M.; Saleemuddin, M. Fibrin matrices: The versatile therapeutic delivery systems. *Int. J. Biol. Macromol.* **2015**, *81*, 121−136.
(64) Koo, J.; Galanakis, D.; Liu, Y.; Ramek, A.; Fields, A.; Ba, X.; Simon, M.; Rafailovich, M. H. Control of anti-thrombogenic properties: surface-induced self-assembly of fibrinogen fibers. *Biomacromolecules* **2012**, *13*, 1259−1268.
(65) Horasawa, N.; Yamashita, T.; Uehara, S.; Udagawa, N. High-performance scaffolds on titanium surfaces: osteoblast differentiation and mineralization promoted by a globular fibrinogen layer through cell-autonomous BMP signaling. *Mater. Sci. Eng., C* **2015**, *46*, 86−96.
(66) Gandhi, J. K.; Knudsen, T.; Hill, M.; Roy, B.; Bachman, L.; Pfannkoch-Andrews, C.; Schmidt, K. N.; Metko, M. M.; Ackerman, M. J.; Resch, Z.; Pulido, J. S.; Marmorstein, A. D. Human Fibrinogen for Maintenance and Differentiation of Induced Pluripotent Stem Cells in Two Dimensions and Three Dimensions. *Stem Cells Transl. Med.* **2019**, *8*, 512−521.
(67) Allan, I. U.; Tolhurst, B. A.; Shevchenko, R. V.; Dainiak, M. B.; Illsley, M.; Ivanov, A.; Jungvid, H.; Galaev, I. Y.; James, S. L.; Mikhalovsky, S. V.; James, S. E. An in vitro evaluation of fibrinogen and gelatin containing cryogels as dermal regeneration scaffolds. *Biomater. Sci.* **2016**, *4*, 1007−1014.
(68) Lei, P.; Padmashali, R. M.; Andreadis, S. T. Cell-controlled and spatially arrayed gene delivery from fibrin hydrogels. *Biomaterials* **2009**, *30*, 3790−3799.
(69) Xie, Y.; Yang, S. T.; Kniss, D. A. Three-dimensional cell-scaffold constructs promote efficient gene transfection: implications for cell-based gene therapy. *Tissue Eng.* **2001**, *7*, 585−598.
(70) Gabarre, S.; Herrera, A.; Ibarz, E.; Mateo, J.; Gil-Albarova, J.; Gracia, L. Comparative Analysis of the Biomechanical Behaviour of Two Cementless Short Stems for Hip Replacement: Linea Anatomic and Minihip. *PLoS One* **2016**, *11*, No. e0158411.
(71) Weissman, D. mRNA transcript therapy. *Expert Rev. Vaccines* **2015**, *14*, 265−281.
(72) Andersson, T.; Agholme, F.; Aspenberg, P.; Tengvall, P. Surface immobilized zoledronate improves screw fixation in rat bone: a new method for the coating of metal implants. *J. Mater. Sci.: Mater. Med.* **2010**, *21*, 3029−3037.
(73) Liu, X.; Tan, N.; Zhou, Y.; Wei, H.; Ren, S.; Yu, F.; Chen, H.; Jia, C.; Yang, G.; Song, Y. Delivery of antagomiR204-conjugated gold nanoparticles from PLGA sheets and its implication in promoting osseointegration of titanium implant in type 2 diabetes mellitus. *Int. J. Nanomed.* **2017**, *12*, 7089−7101.
(74) Jakobsen, T.; Bechtold, J. E.; Søballe, K.; Jensen, T.; Greiner, S.; Vestermark, M. T.; Baas, J. Local delivery of zoledronate from a poly (D,L-lactide)-Coating increases fixation of press-fit implants. *J. Orthop. Res.* **2016**, *34*, 65−71.
(75) Wu, K.; Song, W.; Zhao, L.; Liu, M.; Yan, J.; Andersen, M. Ø.; Kjems, J.; Gao, S.; Zhang, Y. MicroRNA functionalized microporous titanium oxide surface by lyophilization with enhanced osteogenic activity. *ACS Appl. Mater. Interfaces* **2013**, *5*, 2733−2744.

https://dx.doi.org/10.1021/acs.molpharmaceut.0c01042
Mol. Pharmaceutics 2021, 18, 1121−1137